Glycan-Based High-Affinity Ligands for Toxins and Pathogen Receptors

***Ashish A. Kulkarni,*[1] *Alison A. Weiss,*[2] *and Suri S. Iyer*[1]**

[1]UC Chemical and Biosensors Group, Department of Chemistry, University of Cincinnati, Cincinnati, Ohio
[2]Department of Molecular Genetics, Biochemistry and Microbiology, University of Cincinnati, Cincinnati, Ohio

Published online 4 February 2010 in Wiley InterScience (www.interscience.wiley.com).
DOI 10.1002/med.20196

Abstract: Glycans decorate over 95% of the mammalian cell surface in the form of glycolipids and glycoproteins. Several toxins and pathogens bind to these glycans to enter the cells. Understanding the fundamentals of the complex interplay between microbial pathogens and their glycan receptors at the molecular level could lead to the development of novel therapeutics and diagnostics. Using Shiga toxin and influenza virus as examples, we describe the complex biological interface between host glycans and these infectious agents, and recent strategies to develop glycan-based high-affinity ligands. These molecules are expected to ultimately be incorporated into diagnostics and therapeutics, and can be used as probes to study important biological processes. Additionally, by focusing on the specific glycans that microbial pathogens target, we can begin to decipher the "glycocode" and how these glycans participate in normal and aberrant cellular communication. Med Res Rev, 30, No. 2, 327–393, 2010

Key words: shiga; glycan; recognition; influenza; protein–glycan specificity

1. INTRODUCTION

Understanding the "molecular" language used by cells to communicate with each other could lead to strategies to ameliorate a number of diseases processes.[1] The three major classes of biopolymers controlling these communication processes are nucleic acids, proteins, and carbohydrates (or glycans). The 20th century laid the groundwork for understanding nucleic acids and proteins, while glycans remain a challenge for the 21st century. Of these classes of macromolecules, glycans are ubiquitous by virtue of their presence at the front end of the communication signal line, that is, on the surface of cells. Cell-surface glycans, in conjunction with exogenous soluble glycans present in the extracellular matrix, have developed an elaborate "glycocode" to control several biological functions, such as cell adhesion, proliferation,

Contract grant sponsor: NSF; *Contract grant number:* CAREER CHE-0845005; *Contract grant sponsors:* UC Nanotechnology Institute; NIAID; *Contract grant number:* U01-AI075498.

Correspondence to: Suri S. Iyer, UC Chemical and Biosensors Group, Department of Chemistry, Cincinnati, OH 45221-0172, E-mail: suri.iyer@uc.edu

aberrant growth, and organ differentiation.[2–5] The multitude of functions controlled by glycans and the impact of miscommunication requires exquisite control, and glycans have developed a complex language to avoid ambiguity and limit undesired biological outcomes.[3,6]

Like nucleic acids and proteins, glycans use a set of small molecules, specifically monosaccharides, as the "alphabet" to develop their language or the "glycocode." While nucleic acids and amino acids are strung together to produce a linear language that can be directly read, glycan linkage can be nonlinear. The number of permutations and combinations that a few monosaccharide units can achieve far outnumber those afforded by amino acids or nucleotides. For example, two discrete, six carbon monosaccharide units can be linked together in 11 different ways, each with its own unique physicochemical and biological function.[7] By comparison, only one dinucleotide and four dipeptides can be realized from two nucleotides and two amino acids, respectively. In addition to positional isomerism, glycan conformation, density and hydrogen bonding modulate activity of glycans. Several reports have demonstrated that, in addition to the primary structure, density and presentation of glycans can affect binding to its cognate receptor and downstream signaling processes of the glycan.[8–11] The combination of two languages, for example, conjugation of an oligosaccharide to specific proteins, leads to a new dialect and further complexity.[12–16] Despite the enormous complexity, this sophisticated language modulates essential biological functions with clockwork-like precision most of the time. For example, depending on the need, basic fibroblast growth factor, a protein involved in the inflammation and remodeling of the extracellular matrix, interacts with different components of heparan sulfate to promote proliferation or inhibition of cellular growth.[17–19] However, aberrant glycosylation of glycolipids or glycoproteins leads to disease.[20] Clearly, understanding the language of glycans is important to the development of strategies to reverse the irregular or diseased biological state.

2. METHODS FOR STUDYING GLYCAN BIOLOGY

Studies delineating the fundamental physicochemical properties of glycans and their *in vitro* interactions with their cognate receptors allow us to understand how protein–glycan interactions occur at the molecular level. Some of the tools used to study these interactions are glycan/lectin microarrays[21–33] and metabolic engineering.[34–40] Glycan and lectin microarrays are high throughput screening technologies that have been widely used to profile the binding affinities of a number of analytes leading to undiscovered specificities.[22,41–46] Metabolic engineering, which involves the incorporation of unnatural sugars on the cell surface, has shown considerable promise in furthering our understanding of the role of cell-surface glycans. In fact, the visualization of glycans on the cell surface is now possible using these novel technologies. Excellent reviews have been published on the development and application of these novel tools.[24,29,31,35,39,42,47–51]

In addition to these tools, toxins and pathogens are also excellent probes to study the language of glycans. First, toxins/pathogens understand and exploit the specific glycan structures that mammalian cells use to decorate their surfaces (Table I). For example, several toxins and viruses use *N*-acetylneuraminic acids to gain entry into the cell, but use different mechanisms to obtain tissue specificity. Influenza initially binds to terminal *N*-acetylneuraminic acids present on glycoproteins (Table I, B♯ 6,7,8) and glycolipids to gain entry,[52–56] while botulinum toxin initially binds to gangliosides (Table I, A♯ 8,9,10) present on nerve cells until it finds a specific high-affinity protein receptor to enter the cell.[57–59] Second, toxins/pathogens are mutating constantly, leading to a large pool of mutants that possess varying degrees of virulence and glycan-binding affinities. For example, emerging variants of Shiga toxins (Stxs) differ from the parent strains in a few amino acids and seem to prefer different

Table I. Glycan Binding Preferences for Selected Infectious Agents

No.	Bacterial toxins/ lectins	Protein structure	Glycan receptor	Method	Data obtained
A. Toxins					
1	Cholera toxin	AB_5 type, A—toxic part, B_5—five identical binding subunits	GM1 pentasaccharide GM1 pentasaccharide mimics GM1pentasaccharide; GM2 tetrasaccharide; Galβ(1,3)GalNAcβOMe; Neu5AcαOMe; GalβOMe; GM3 trisaccharide; GalNAcβOMe GM1; GD1b	Crystal structure (PDB ID: 2CHB, 3CHB) NMR spectroscopy Fluorescence titration experiments ITC SPR	Molecular level interactions[221–223] Molecular level interactions[224] $K_d = 0.1–10 \times 10^{-8}$ M[224] GM1: $K_d = 43 \times 10^{-9}$ M, GM2–GalNAcβOMe: $K_d = 2–210 \times 10^{-3}$ M[225] GM1: $K_d = 0.73 \times 10^{-9}$ M, GD1b: $K_d = 8.0 \times 10^{-9}$ M[226]
2	Heat labile enterotoxin	AB_5 type, A—toxic part, B_5—five identical binding subunits	Galβ(1,4)Glc GalNAcα(1,3)Fucα(1,2) Galβ-(1,4) Fucα(1,3)Glcβ GM1; GD1b; Asialo-GM1	Crystal structure (PDB ID: 1LTT) Crystal structure (PDB ID: 202L) Binding is not in a regular binding site SPR	Molecular level interactions[227] Molecular level interactions[228] GM1: $K_d = 0.57 \times 10^{-9}$ M, GD1b : $K_d = 3 \times 10^{-9}$ M, Asialo-GM1: $K_d = 15 \times 10^{-9}$ M[226]
3	Pertussis toxin	AB_5 type, A—toxic part, B_5—subunits are not identical	Neu5Acα(2,6)Gal Multiantennary *N*-glycans and glycoproteins	Crystal structure (PDB ID: 1PTO) Screening by ELISA	Molecular level interactions[229] Qualitative[230]

Table I. Continued

No.	Bacterial toxins/ lectins	Protein structure	Glycan receptor	Method	Data obtained
4	Subtilase cytotoxin	AB_5 type, A—toxic part, B_5—five binding subunits	Neu5Gcα(2,3)Galβ(1,4) GlcNAc; Neu5Gcα(2,3)Galβ(1,4) Glc; Neu5Acα	Glycan array Crystal structure (PDB ID: 3DWP, 3DWQ) Cytotoxicity assay Inhibition studies	Qualitative[34] Molecular level interactions[34] Neu5Gc: $CD_{50} = 3.92 \pm 1.58$ pg for human breast cancer MDA-Mb-231 cells $CD_{50} = 1.33 \pm 0.3$ pg for human embryonic kidney 293 cells Neu5Ac: $CD_{50} = 13.17 \pm 2.46$ pg human breast cancer MDA-Mb-231 cells $CD_{50} = 11.58 \pm 3.30$ pg for human embryonic kidney 293 cells Neu5Gcα(2,3)Galβ(1,4)Glc: $K_i = 2 \times 10^{-3}$ M
5	Shiga toxin 1	AB_5 type, A—toxic part, B_5-—five identical binding subunits	Glycolipids Galα(1,4)Galβ(1,4)Glc (Pk trisaccharide) derivatives Starfish® Pk trisaccharide containing copolymers	Screening by chromatogram-binding assay Crystal structure (PDB ID: 1BOS) ELISA Crystal structure (PDB ID: 1QNU) Neutralization assay	Qualitative[231] Molecular level interactions[216] $IC_{50} = 0.4 \times 10^{-9}$ M[127] Molecular level interactions[127] $IC_{50} = 0.58–6.89 \times 10^{-7}$ M[145]
6	Shiga toxin 2	AB_5 type, A—toxic part, B_5—five identical binding subunits	Gb3 GalNAcα(1,4) Galβ(1,4)Glc Starfish® Pk trisaccharide containing	TLC overlay assay ELISA using streptavidin–biotin conjugation platform ELISA	Qualitative[232] Qualitative[155] $IC_{50} = 6 \times 10^{-9}$ M[127] $IC_{50} = 0.19–24.3 \times 10^{-6}$ M[145]

			copolymers Lipopolysaccharides from *E. coli* O107/117	Neutralization assay Neutralization assay using vero cells	Stx1: no inhibition Stx2: significant inhibition[233]
7	Tetanus toxin	AB type, A—toxic part, B—binding subunit	Neu5Acα(2,8)Neu5Acα (2,3)Galβ(1,4)Glc Galβ (1,4)Glc; Neu5Ac GT1b mimics GD1b, GT1b Neu5Acα(2–6)Gal; Neu5Acα (2,8)Neu5Acα(2,3)Galβ (1,4)Glc; $(Neu5Ac)_n$ oligomers $n = 1–6$	Crystal structure (PDB ID: 1YXW) Crystal structure (PDB ID: 1D0H) Crystal structure (PDB ID: 1FV2) SPR Mass spectroscopy	Molecular level interactions[234] Molecular level interactions[235] Molecular level interactions[236] GD1b: $K_d = 0.15 \times 10^{-6}$ M, GT1b: $K_d = 0.17 \times 10^{-6}$ M[226] $K_d = 10–35 \times 10^{-6}$ M[237]
8	Botulinum toxin A and E	AB type, A—toxic part, B—binding subunit	GT1b	Crystal structure (PDB ID: 2VUA)	Molecular level interactions[238]
9	Botulinum toxin B	AB type, A—toxic part, B—binding subunit	Neu5Acα(2,3)Galβ(1,4)Glc	Crystal structure (PDB ID: 1EPW)	Molecular level interactions[239]
10	Botulinum toxin C (C16S), HA1 from progenitor toxin	Several hemagglutinin (HA) subcomponents in addition to the 12S toxin component	Neu5Ac; GalNAc	Crystal structure (PDB ID: 1YBI)	Molecular level interactions[240]
11	*Clostridium difficile* toxin A	3 regions; *N*-terminal region, translocating region, *C*-terminal region	Galα (1,3)Galβ(1,4) GlcNAcβ $O(CH_2)_8CO_2CH_3$ Galβ(1,4)[Fucα(1,3)] GlcNAcβ(1,3)Galβ(1,4) Glc; [Fucα(1,2)]Galβ(1,4) [Fucα(1,3)] GlcNAcβ1; Galβ(1,4) GlcNAcβ(1,3) [Galβ(1,4)GlcNAcβ (1,6)] Galβ (1,4)Glc	Crystal structure (PDB ID: 2G7C) ELISA, affinity chromatography	Molecular level interactions[241] Qualitative[242]

Table I. Continued

No.	Bacterial toxins/ lectins	Protein structure	Glycan receptor	Method	Data obtained
12	Staphylococcal enterotoxin	Two domains, *N*-terminus domain and *C*-terminus domain	Neu5Acα(2,3) Galβ(1,4)Glc Sialyl Lewis X Sialyl Lewis X	Crystal structure (PDB ID: 1SE3) Crystal structure (PDB ID: 2RDG) Crystal structure (PDB ID: 2Z8L, 2R61)	Molecular level interactions[243] Molecular level interactions[244] Molecular level interactions[245]
13	*Pseudomonas aeruginosa* lectin I(PA IL)	Tetramer	α Gal derivatives, Galα(1,4)Gal; Gb3; iGb3 Galactose	Glycan array ITC Crystal structure (PDB ID: 2VXJ) Crystal structure (PDB ID: 1OKO)	Qualitative[246] iGb3: $K_d = 68 \times 10^{-6}$ M, Gb3: $K_d = 77 \times 10^{-6}$ M[246] Molecular level interactions[246] Molecular level interactions[247]
14	*Burkholderia cenocepacia* lectin A (BclA)	Homodimers	Man-α-OMe mimics	Glycan array SPR Crystal structure (PDB ID: 2VNV)	Qualitative[248] Man-α-OMe: $K_d = 2.75 \times 10^{-6}$ M[248] Molecular level interactions[248]
15	*Chromobacterium Violaceum* lectin II (CV-IIL)	Tetramer	Man-α-OMe mimics; Fuc-α-OMe mimics Lewis a trisaccharide	ITC Crystal structure (PDB ID: 2BV4) Crystal structure (PDB ID: 1W8H)	Man-α-OMe: $K_d = 19 \times 10^{-6}$ M Fuc-α-OMe: $K_d = 1.7 \times 10^{-6}$ M[249] Molecular level interactions[249] Molecular level interactions[250]
16	*Pseudomonas aeruginosa* lectin II(PA IIL)	Tetramer	α-Fuc derivatives; α-Fuc	Crystal structure (PDB ID: 1GZT) Inhibition studies	Molecular level interactions[251] $IC_{50} = 0.05–6.0 \times 10^{-9}$ M[251]
17	*Ralstonia solanacearum* lectin II (RS-IIL)	Tetramer	Man-α-OMe derivatives	Hemagglutination inhibition assay Crystal structure (PDB ID: 1UQX)	Qualitative[252] Molecular level interactions[252]

B. Viruses

No.	Virus	Protein on virus	Glycan receptor	Method	Data obtained
1	Norovirus	Capsid protein (VP1): shell S domain and P domain with dimeric subdomains involved in carbohydrate binding	GalNAcα(1,3)[Fuc α(1,2)] Galβ(1,3)GlcNAc Sialyl LewisX Sialyl diLewisX [Fuc α(1,2)]Galβ(1,3)GlcNAcβ (1,3)Galβ(1,4)Glc; GalNAcα(1,3)[Fuc α(1,2)] Galβ(1,3)GlcNAc [Fuc α(1,2)]Galβ(1,3)GlcNAcβ (1,3)Galβ(1,4)Glc; [Fuc α(1,2)]Galβ(1,3)[Fuc α(1,4)]GlcNAcβ (1,3)Galβ [Fucα(1,2)] GalNAcα(1,3)Gal; [Fucα (1,2)]Galα(1–3)Gal	Crystal structure (PDB ID: 3BYI), NV-GI-1 strain ELISA Crystal structure(PDB ID: 2ZL6, 2ZL7), NV-GI-1 strain Magnetic bead–virus capture method Crystal structure (PDB ID: 2OBS, 2OBT), NV-GII-4 strain, VA387	Molecular level interactions[253] Qualitative[254] Molecular level interactions[255] Qualitative[256] Molecular level interactions[257]
2	Rotavirus	Protein spikes of VP4 virion-associated subunits VP8* and VP5*	Neu5Acα(2–3)Galβ(1,4)Glc; Neu5Acα2Me Neu5Ac; Neu5Acα2Me Neu5Acα2Me Neu5Ac mimetics	Crystal structure (PDB ID: 2DWR, 2I2S), WA and CRW-8 strains Crystal structure (PDB ID: 1KQR) Crystal structure (PDB ID: 2P3K, 2P3I, 2P3J) RRV VP8* STD NMR ITC Neutralization assays	Molecular level interactions[258] Molecular level interactions[259] Molecular level interactions[260] Molecular level interactions[260] $K_d = 0.33 \times 10^{-3}$ M[260] $IC_{50} = 6.25–25 \times 10^{-3}$ M[261]
3	Foot-and-mouth disease virus	Capsid proteins (VP1, VP2, VP3)	Heparan sulfate	Crystal structure (PDB ID: 1QQP)	Molecular level interactions[262]

Table I. Continued

No.	Virus	Protein on virus	Glycan receptor	Method	Data obtained
4	Murine polyomavirus	VP1: pentamer	Neu5Acα(2,3)Galβ(1,3) GalNAc; Neu5Acα(2,3)Galβ(1,3) [Neu5Acα(2,6)] GlcNAcβ(1,3) Galβ(1,4) Neu5Acα(2,3) Galβ(1,4)Glc; Neu5Acα(2,3)Galβ(1,3) [Neu5Acα(2,6)] GlcNAc	Crystal structure (PDB ID: 1VPS) Crystal structure (PDB ID: 1SID, 1SIE)	Molecular level interactions[263] Molecular level interactions[264]
5	Adenovirus (AD37 and AD19p)	Fibre proteins: trimer	Neu5Acα (2,3) Galβ(1,4)Glc HAS conjugates of Neu5Ac α (2,3) Gal β (1,4)Glc	Crystal structure (PDB ID: AD37- 1UXA, AD19p- 1UXB) Inhibition assay	AD37: $K_d = 5 \times 10^{-3}$ M, AD 19p: $K_d = 7 \times 10^{-3}$ M[265] Qualitative[266]
6	Influenza virus A (human). Note: Only selected strains are indicated in this entry. More examples can be found in tables 4 and 5.	Hemagglutinin protein (H1): trimer; Neuraminidase: tetramer	Neu5Ac α(2,6) Neu5Ac derivatives Neu5Acα(2,3)$_n$[Galβ (1,4)Glcβ(1,4)]$_4$Cer; Neu5Acα(2,6)$_n$[Galβ(1,4) Glcβ(1,4)]$_4$Cer NeuAcα(2,6)Galβ(1,4) G lcNAcβ(1,3)Galβ(1,4)Glc; NeuAcα (2,3)Galβ (1,3) GlcNAcβ(1,3)Galβ(1,4) Glc NeuAcα(2,6)Galβ(1,4)G lcNAcβ(1,3)Galβ(1,4)Glc; NeuAcα (2,3)Galβ (1,3) GlcNAcβ(1,3)Galβ(1,4) Glc NeuAcα(2,6)Galβ(1,4)G lcNAcβ(1,3)Galβ(1,4)Glc;	Hemagglutination assay NMR, crystal structure (PDB ID: 1HGD–1HGJ), X-31 strain SPR Crystal structure, (PDB ID: 1JSH, 1JSI) A/swine/Hong Kong/9/98 ; (PDB ID: 1JSN, 1JSO) A/Duck/Singapore/3/97 Crystal structure (PDB ID: 1RUZ) 1918 human, (PDB ID: 1RU7, 1RVZ, 1RVX) 1934 human, (PDB ID: 1RUY, 1RVT, 1RV0) 1930 swine Crystal structure, (PDB ID: 3HTP, 3HTQ, 3HTT) WDK/JX/12416/2005	Qualitative[267] $K_d = 1.4–22 \times 10^{-9}$ M[219] Neu5Acα(2,3): $K_d = 0.195 \times 10^{-9}$ M Neu5Acα(2,6): $K_d = 0.032 \times 10^{-9}$ M[268] Molecular level interactions[56] Molecular level interactions[269] Molecular level interactions[270]
7	Influenza virus B	Hemagglutinin protein: trimer; Neuraminidase: Tetramer	NeuAcα(2,6)Galβ(1,4)G lcNAcβ(1,3)Galβ(1,4)Glc; NeuAcα (2,3)Galβ (1,3) GlcNAcβ(1,3)Galβ(1,4) Glc	Crystal structure (PDB ID: 2RFT, 2RFU), B/Hongkong/8/73 strain	Molecular level interactions[271]

8	Influenza virus C	Hemagglutinin protein: trimer; Neuraminidase: tetramer	Neu5,7Ac_2-GD3; Neu5,7,9Ac_3-GD3	HPTLC overlay assay, solid-phase assay, inhibition assay	Qualitative[272]
10	Rubivirus	Spike proteins	Unidentified glycoproteins	Inhibition assays	Qualitative[273]
11	Paramyxovirus	Hemagglutinin protein: dimer	Neu5Acα(2,3)Gal β (1,3)GalNAc; Neu5Acα(2,8)Neu5Ac α(2,3)Galβ(1,3)GalNAc; GD1a	^{31}P NMR	Qualitative[274]
12	Newcastle disease virus	Hemagglutinin–neuraminidase protein: dimer	Neu5Acα(2,3)Galβ(1,3) GalNAc	Lectin column chromatography and reversed-phase high-performance liquid chromatography	Qualitative[275]
13	Simian virus	SV40 capsid protein, VP1:pentamer	GM1	Crystal structure (PDB ID: 3BWR), SV40 strain ITC Glycan array	Molecular level interactions[276] $K_d = 1–5 \times 10^{-3}$ M[276] Qualitative[276,277]

C. Bacteria

No.	Bacterium	Protein on bacterium	Glycan receptor	Method	Data obtained
1	*Streptococcus suis*	Digalactose-binding adhesion protein	Galα(1,4)Galβ-OMe; 2-Deoxy-Galα(1,4)Galβ-OMe 3-OMe-Galα(1,4)Galβ-OMe 3-Deoxy-Galα(1,4)Galβ-OMe 6-Deoxy-Galα(1,4)Galβ-OMe Galα(1,4)-2-deoxy-Galβ-OMe Galα(1,4)-3-deoxy-Galβ-OMe Galα(1,4)-3-C-Me-Galβ-OMe Galα(1,4)-4-deoxy-Galβ-OMe Galα(1,4)-6-deoxy-Galβ-OMe Galα(1,4)Galβ-*O*-$(CH_2)_2SiMe_3$ GalNAcβ(1,3)Galα(1,4) Galβ4-0-$(CH_2)_2SiMe_3$	Inhibition assay	*S. suis* P_N: $IC_{50} = 0.059–2.5 \times 10^{-3}$ M *S. suis* P_O: $IC_{50} = 0.016–2.5 \times 10^{-3}$ M[63]

Table I. Continued

No.	Bacterium	Protein on bacterium	Glycan receptor	Method	Data obtained
2	Enteroaggregative *E. coli*	Hemagglutinin	Neu5Ac Neu5Ac derivatives	HA inhibition assay	Qualitative[278]
3	P-fimbriated *E. coli*	PapG adhesion: digalactose-binding monomer on the P pili	Galα (1,4)Galβ Galα (1,4)Gal GbO4	Crystal structure (PDB ID: 1J8S)	Qualitative[279] Molecular level interactions[280]
4	S-fimbriated *E. coli*	S fimbriae: Neu5Acα2–3 galactoside-binding monmer on bacterial fimbriae	NeuGcα(2,3)Gal; Neu5Acα(2,8)Neu5Ac; sialoglycoproteins and sialogangliosides	Solid phase HA inhibition and ELISA assays	Qualitative[281]
5	Uropathogenic *E. coli* (Type 1 pili)	FimH: mannose-binding monomer	Man α derivatives; Mannose containing glycoproteins	Aggregation assay Crystal structure PDB ID: 2VCO, 1KIU, 1KLF)	Qualitative[282] Molecular level interactions[283,284]
6	*Actinomyces naeslundii* 12104 and A. viscosus LY7	Type 2 fimbriae: GalNAcβ-binding monomer on the pili structure	GalNAcβ(1,4)Galβ(1,4)GlcCer; Galβ(1,4)GalNAcβ(1,4)Galβ (1,4)GlcCer; GalNAcβ(1,3)Galα(1,3)Galβ (1,4)GlcCer; GalNAcβ(1,3)Galα(1,4)Galβ (1,4)GlcCer; GalNAcβ(1,3)GalNAcβ(1,3) Galα(1,4)Galβ(1,4)GlcCer; Galβ(1,3)GalNAcβ(1,3)Galα (1,4)Gal; Glcβ(1,4)Cer; Galβ(1,3)(NeuAcα2–6) ; GalNAcβ(1,4)Galβ(1,4) GlcCer	HA inhibition assays	Qualitative[285]
7	*Helicobacter pylori*	Hemagglutinin and fucose sensitive receptor	Lewis(b) blood group antigen	Protein immunoblots	Qualitative[286]

8	*Helicobacter pylori*	Laminin-binding protein	Neu5Acα(2,3) derivatives	HA inhibition assay	Qualitative[287]
9	*Mycoplasma pneumoniae*	Protein (40 and 90 kDa) on the tips of the pili	Long-chain Neu5Ac oligosaccharides		
10	*Mycoplasma bovis*	Protein (26 kDa)	NeuAcα(2,6)Galβ(1,4)Glc; glycophorin, dextran sulfate	Adherence inhibition assay	Qualitative[288]
11	*Porphyromonas (Bacteroides) gingivalis*	P. gingivalis Fimbriae: *N*-acetyl-D-galactosamine-binding monomer on the pili structure	Galβ(1,4)GalNAc	Inhibition assay	Qualitative[289]
12	*Pseudomonas aeruginosa*	Pilus adhesion: lactose-binding monomer on pili structure	Galβ(1,3)GalNAcβ(1,4)Galβ(1,4)Glcβ(1,1)Cer; Galβ(1,4)Glc; Galβ(1,4)Glcβ(1,3)Fuc; Galβ(1,4)GlcNAcβ(1,3)Galβ(1,4)Glc; Galβ(1,3)GlcNAcβ(1,3)Galβ(1,4)Glc; GalNAcβ(1,4) in asialo-GM1 and asialo-GM2	Chromatogram overlay assay	Qualitative[290]
13	*Rhizobium lupini*	L-fucose-binding protein	L-αFuc	Aggregation and fluorescent assays	Qualitative[291]

Note: GM1, Galβ(1,3)GalNAcβ(1,4)[NeuAcα(2,3)]Galβ(1,4)Glcβ(1,1)ceramide; GM2, GalNAcβ(1,4)[NeuAcα(2,3)]Galβ(1,4)Glcβ(1,1)ceramide; GM3, NeuAcα(2,3)Galβ(1,4)Glcβ(1,1)ceramide; GD1b, Galβ(1,3)GalNAcβ(1,4)[NeuAcα(2,8)NeuAcα(2,3)]Galβ(1,4)Glcβ(1,1)ceramide; Asialo GM1, Galβ(1,3)GalNAcβ(1,4)Galβ(1,4)Glcβ(1,1)ceramide; Gb3, Galα(1,4)-Galβ(1,4)Glcβ(1,1)ceramide; iGb3, Galα(1,3)Galβ(1,4)Glcβ(1,1)ceramide; GT1b, NeuAcα(2,3)Galβ(1,3)GalNAcβ(1,4)[NeuAcα(2,8)NeuAcα(2,3)]Galβ(1,4)Glcβ(1,1)ceramide; Sialyl LewisX, Neu5Acα(2,3)Galβ(1,4)[Fucα(1,3)]GlcNAcβ(1,3)Galβ(1,4)Glc(1,1)ceramide; Sialyl diLewisX, Neu5Acα(2,3)Galβ(1,4)[Fucα(1,3)]GlcNAcβ(1,3)Galβ(1,4)[Fucα(1,3)]GlcNAcβ(1,3)Galβ(1,4)Glc(1,1)ceramide; Lewis (b) blood group antigen, Fucα(1,2)Galβ(1,3)[Fucα(1,4)]GlcNAcβ(1,3)Galβ(1,4)Glc GbO4, GalNAcβ(1,3)Galα(1,4)Galβ(1,4)Glcβ(1,1)ceramide.

glycans for binding.[8,60] More importantly, these emerging variants differ significantly in their ability to cause disease, as evidenced in animal model[60,61] and epidemiological studies.[62] Thus, infectious agents are excellent probes to understand the molecular basis of glycan–-protein specificity and to correlate *in vitro* glycan binding to *in vivo* biological function, the latter being one of the significant research gaps in the field of glycoscience.

3. FACTORS THAT INFLUENCE RECEPTOR RECOGNITION

When compared to genomics or proteomics, glycan recognition is considerably more complicated. The interaction of a toxin/pathogen with its cognate glycan receptor is dependent on several factors. We discuss three factors that play an important role in determining whether a specific glycan will serve as a receptor for a microbial pathogen: primary structure of the glycan, glycan presentation, and density of the glycan on the cell surface.

A. Primary Structure

The primary structure of the glycan remains the most important factor in determining pathogen/host interactions. It is clear from Table I that, in addition to broad glycan preferences, different toxins or pathogens can exhibit binding to the same glycan, leading to the incorrect assumption of lack of specificity. While a particular glycan is capable of binding different microbes, the mechanisms can be different and can be exploited to achieve requisite specificity. For example, the common receptor for *Streptococcus suis* (Table I, C♯ 1) and P fimbriated *Escherichia coli* (Table I, C♯ 3) is the naturally occurring Gal(α1–4)Gal disaccharide. In pioneering studies, it was shown that these two distinct pathogens bind to different parts of the same disaccharide. Briefly, a panel of compounds related to the Gal(α1–4)Gal epitope, such as 4′ deoxy Gal(α1–4)Gal, 4′′ deoxy Gal (α1–4)Gal, 3′ deoxy Gal(α1–4)Gal, were chemically synthesized and evaluated for binding using a hemagglutination inhibition assay.[63] The essential hydroxyls for binding to two groups of *S. suis* were the 4′ OH, 6′ OH, 2 OH, and 3 OH, whereas P fimbriated *E. coli* binds to a cluster of five hydroxyls (6 OH, 2′ OH, 3′ OH, 4′ OH, and 6′ OH) on the opposite side (Fig. 1). Thus, *S. suis* and P fimbriated *E. coli* bind to different parts of the same disaccharide receptor. Within a toxin/pathogen family, the binding preferences of different variants can be different with the internal sugars exerting their influence in the recognition process (discussed later in the Shiga and influenza subsections).

It is worth mentioning that the field of glycan–toxin/pathogen interactions is still in its infancy and elaborate structure activity relationship studies, such as the one described above,

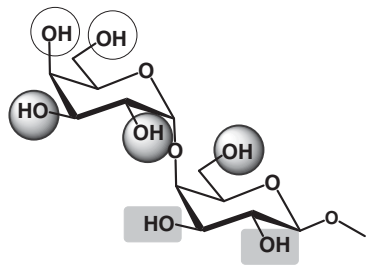

Figure 1. Gal (α1,4). Gal residue that binds to *Streptococcus suis* and *P. fimbriated E. coli.* Hydroxyl functionalities that bind exclusively to *S. suis* and *P. fimbriated E. coli* are shaded in medium gray circle and dark gray rectangles, respectively. Hydroxyls critical to both pathogens are indicated using open circles.

are limited. The earliest studies assessed binding to monosaccharides and were typically limited to qualitative analysis. However, it is increasingly being recognized that most glycan-binding proteins recognize structures that are more complex than a monosaccharide, and quantitative analyses are now emerging.

Studies on protein binding to more complex glycans have been limited, primarily because the synthesis of ultra pure synthetic glycans has been time consuming and labor intensive in the past. However, novel methodologies, such as solid phase,[64–79] 1-pot,[80–93] and enzyme-based technologies[94–110] have significantly alleviated the problem of rapid production of glycans significantly. Thus, Table I represents only a small subset of the vast number of potential interactions between infectious agents and glycans. As the field evolves, it is anticipated that broad preferences will be narrowed down to specific binding motifs, which can be used to develop lead compounds for glycan-based therapeutics and diagnostics.

B. Glycan Density

It is well known that protein–monosaccharide interactions are generally rather weak, typically in the millimolar range. High-affinity binding is achieved through multivalent interactions. It is imperative to note that just increasing the glycan density is not sufficient to obtain the desired signaling as the protein density on the pathogen; the number of binding sites and distance between binding sites on the protein have been shown to significantly affect binding affinities.[11,111,112] Toxins and pathogens use different strategies to achieve multivalency. For example, the tip of each Type 1 pilus of *E. coli* possesses a single mannose-binding protein (Table I, C♯ 5). Multiple receptors must be engaged to mediate stable bacterial attachment; however, the bacteria elaborate hundreds of long flexible pili, which can accommodate sparse or uneven receptor distribution on the host cell (Fig. 2A). In contrast, the glycan-binding proteins of viruses are densely packed. Influenza virus attachment is mediated by the hemagglutinin (HA) trimer (Fig. 2B, shown in yellow), although tetrameric neuraminidase (NA) (Fig. 2B, shown in red) may also participate in the attachment. Each HA protein is a trimer, capable of engaging three molecules of sialic acid, and the surface of each virion contains many copies of the HA protein. The small size and relatively inflexible nature of the virion may demand certain patterns of receptor distribution; however, this has yet to be investigated. Receptor density may have the strongest influence on susceptibility to bacterial toxins. Shiga toxin (Stx) attachment is mediated by a pentamer of five identical protein subunits, and densely packed receptor distribution is critical for binding. (Fig. 2C). Overall, the structure of the glycan and the density play an important role in the recognition event. In some cases, such as Stxs, densely packed receptors are needed for binding, while in other cases, such as *E. coli*, sparsely populated glycans can still result in infection.

C. Glycan Presentation

Recognition of the glycan can also be influenced by how it is displayed on the cell surface. Unlike most proteins, glycans adopt several thermodynamically stable conformations, and the ability of a glycan to adopt the conformation needed for receptor recognition can be influenced by adjacent residues that play a limited role in the recognition process. In several instances, the correct glycan conformation is induced *when* the protein interacts with the glycan.[113–115] Tethering glycans to a surface can limit the number of conformations, and it has been well established that glycans-on-a-surface exhibit different binding affinities toward the same protein than free glycans-in-solution. Thus, binding studies using ELISA and SPR techniques, where one of the components is tethered to the surface, may differ from ITC or NMR techniques, where both components are in solution.[116,117] The advantages and

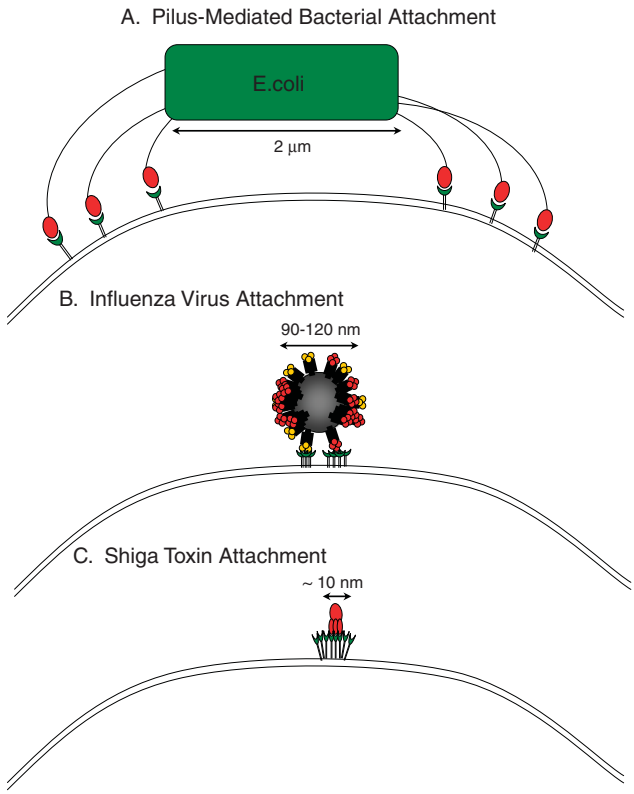

Figure 2. Influence of glycan distribution on binding of toxins, viruses, and pathogens. [Color figure can be viewed in the online issue, which is available at www.interscience.wiley.com.]

shortcomings of some of the techniques are presented in Table II. Also, binding is influenced by the spacers that connect the glycans to the surface; shorter spacers can result in limited conformations compared to longer spacers. However, if the spacers are too long, it may result in decreased binding due to loss in multivalency. Overall, improperly presented glycans can fail to bind to the protein and give false negatives, and this could have implications in the interpretation of glycan microarray results.

We describe the interaction of two well-studied systems, Stx and influenza virus, with host glycans, and efforts to inhibit the infection process in the following sections.

4. SHIGA TOXIN

Stx is the major virulence factor of several Gram negative bacteria, including *E. coli* and *Shigella dysenteriae*.[118] Stx-related food-borne illness affects over 70,000 people in the United States annually, with children under the age of five and the elderly being the most susceptible.[118–120] Contamination with Stx-producing *E. coli O157:H7* is a constant threat to our food, drinking water, and recreational waters. The symptoms include severe abdominal cramping, watery and bloody diarrhea. Spontaneous resolution is observed in 85–90% of all cases. However, 10–15% of patients are severely affected and develop hemolytic uremic syndrome (HUS), kidney failure, and possibly death. Antibiotic treatment is contraindicated because it can promote progression to severe disease by increasing Stx production, and treatment is mainly supportive.[121]

Table II. Salient Features of Different Biophysical Techniques for Quantitative Binding Analysis

	Advantages	Other considerations
Glycans on surface		
ELISA	(i) High throughput screening (ii) Dose response studies give apparent K_d's (iii) Incubation time studies identify highest affinity ligands for dynamic systems[11] (iv) Limited amounts of glycan and protein required	(i) Results dependent on glycan spacer, density, and architecture (ii) Requires labeled detection reagents (antibodies)
SPR	(i) Newer instruments are capable of high throughput screening (ii) Kinetic data such as ON/OFF rates are obtained, which are highly relevant to in vivo biological function (iii) Label-free technique (iv) Glycan on chip can assess multivalent interactions; protein on chip can assess monovalent interactions (v) Limited amounts of glycan and protein are required (vi) Use of the appropriate (such as a lipid bilayer) sensor chip can mimic biological system	(i) Results dependent on glycan spacer, density, and architecture (ii) Algorithms for analysis only developed for bivalent systems, only apparent Kd can be obtained for multivalent–multivalent interactions
Glycans in solution		
Saturation Transfer Difference (STD) NMR Spectroscopy	(i) Identification of part of the glycan that binds to the protein (ii) Competition experiments between two glycans will identify the higher affinity glycan (iii) Quantitative K_d for nonmultivalent systems (iv) Label-free technique	(i) Multivalent systems are more difficult to analyze (ii) No information of the binding site of the protein unless the protein is labeled (iii) Large amounts of analytes are required (iv) Not a true representation of the interactions at the cell surface
ITC	(i) Thermodynamic data are obtained, which are highly relevant to in vivo biological function, especially when glycans in solution are being studied (ii) Label-free technique	(i) Multivalent systems are more difficult to analyze (ii) Large amounts of analytes are required (iii) Not a true representation of the interactions at the cell surface, that is, glycans-on-a-solid surface cannot be assayed using ITC, as both components need to be solution

Among the Stx producing *E. coli* strains, O157:H7 is the predominant serotype found in the United States. Strains of *E. coli* O157:H7 can produce Stx1, Stx2, or both, but severe disease is most commonly associated with strains that produce the more potent toxin variant, Stx2. While most common *E. coli* serotypes do not produce Stx, Stxs are encoded on lysogenic bacteriophage, and can be transmitted to other serotypes of *E. coli* and even other enteric bacterial species. Indeed, it has been shown that other strains, such as O26, O146, O103, and O117, can produce Stx, as can commensal strains.[122] Because several serotypes besides O157:H7 can produce Stx, the CDC recommends testing clinical isolates for Stx production instead of screening for the presence of the O157:H7 serotype.[123]

Stx belongs to the AB_5 family of toxins that include cholera toxin (Table I, A♯ 1), heat labile toxin (Table I, A♯ 2), pertussis toxin (Table I, A♯ 3), and subtilase toxin (Table I A♯ 4). The five B subunits in Stx are identical. The A subunit possesses the toxic activity and cleaves a single adenine residue from the 28S ribosomal RNA molecule, thereby inactivating the ribosome and halting protein synthesis. It is very interesting that a similar *N*-glycosidase activity is observed with the plant toxin ricin, another biothreat agent. However, ricin binds to galactose or galactosamine monosaccharides as a receptor, whereas Stx requires disaccharides or trisaccharides to bind effectively.[124] Also, ricin appears to target the liver, whereas Stx causes HUS and kidney failure. Thus, although both toxins affect the ribosome, the different receptor preferences lead to different pathologies.

A. Clustering of Glycans Dramatically Increases the Affinity of Shiga Toxins

The structure of Stxs are shown in Figure 3. The five identical B, or binding subunits of Stx, forms a pentamer with superficial pentaradial symmetry, similar to the shape of a starfish. The A subunit sits in the pocket formed at the center of the B pentamer.[125] The details of the molecular basis of receptor recognition have been most fully developed for Stx1. Each B subunit of Stx1 has three binding sites, of which site 2 has been shown to be the most important (Fig. 3B).[126,127] Multiple studies have demonstrated that the functional receptor for Stx1 is a neutral glycolipid, globotriaosylceramide (Gb3), shown in Figure 4A,[128–131] and Stx binds to the glycan head group of Gb3, also known as the Pk trisaccharide. A single trisaccharide binds with millimolar affinity to Stx, which is typical of most glycan–protein interactions. However, when multiple copies of the receptor are arrayed on a surface, similar to how they are presented on the cell membrane, the toxin is able to engage multiple receptors and the binding affinity increases dramatically (Table III).[127]

Several synthetic analogues comprising of the Pk trisaccharide linked to various scaffolds have been synthesized and assayed for binding with Stxs. The general theme of all these synthetic molecules is that increased affinity is achieved by increasing the number of glycans displayed to maximize accessibility to the toxin-binding sites[132–147] (Table III). A single Pk trisaccharide exhibits millimolar-binding affinity which increases to a micromolar-binding affinity in bivalent molecules (Table III, entry ♯ 5). When the Pk trisaccharides are tethered to a multivalent scaffold designed to engage all the binding sites of the toxin, such as the Starfish® and Daisy® ligands (Table III, entry ♯ 17) developed in seminal studies by Bundle and co-workers, subnanomolar affinities can be obtained.[127] It is important to note that the design of the dendrimeric scaffold is crucial to achieving high affinities, as some of the silane-based dendrimers (Table III, entries 13–15) exhibit lower binding affinities when compared to the Starfish® ligand. Alternatives to the dendrimer scaffolds are polymeric constructs, where the Pk trisaccharides are dangling from the main branch of the polymer (Table III, entries 6–12). Several of these polymeric molecules are depicted in Table III, and glycans with appropriate spacers conforming to the binding sites also exhibit subnanomolar binding affinities toward Stx. More recently, an *in vivo* supramolecular templating strategy has been

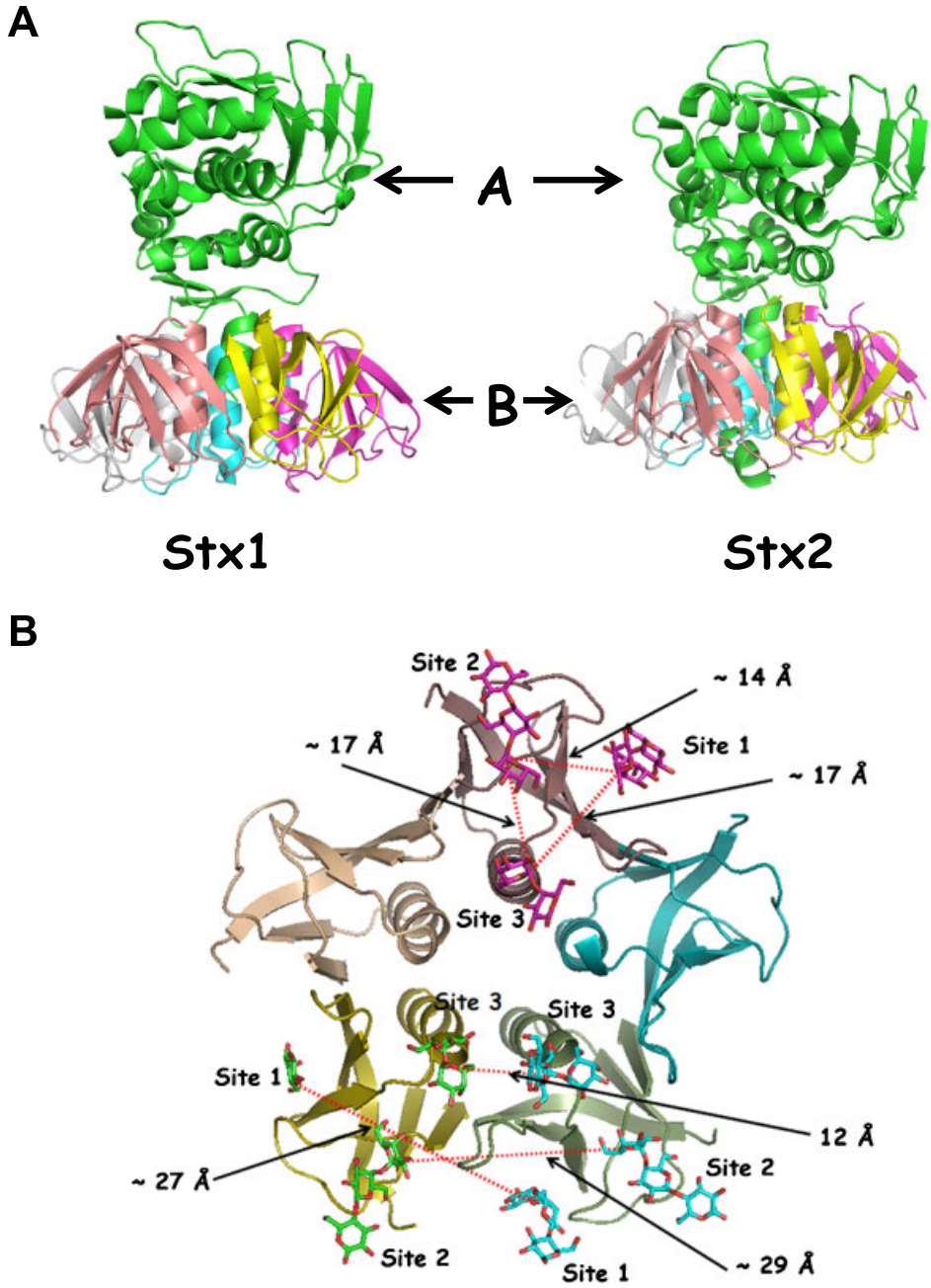

Figure 3. (**A**) Side view of ribbon diagram of Stx1 and Stx2. The enzymatically active A-subunit is shown in green. The binding or B-subunit is a pentamer of five identical subunits, each displayed in a different color in this representation. The receptor binding domains are on the bottom of the B-pentamer[214,215] (PDB ID: Stx1 - 1DM0, Stx2 - 1R4Q). (**B**) Top view representation of Stx1 homo-pentamer. The structures were downloaded from NCBI and the figures were generated using Pymol® software (PDB ID: 1BOS).[216] Figure has been adapted with permission from reference (Publisher: Wiley Interscience).[217]

used to design high-affinity ligands leading to effective neutralization of Stx in animal models.[148] This strategy involves the use of an endogenous HuSAP protein, a homopentamer with a structure similar to the Stx B-pentamer, which binds to pyruvate acetals of glycerol.

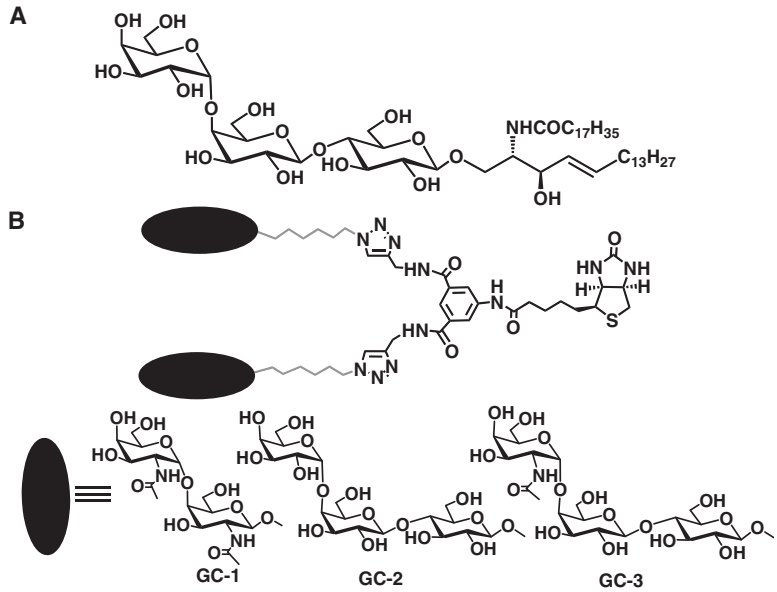

Figure 4. (**A**) Structure of Gb3. (**B**) Structures of the synthetic molecules that differentiate between Stx1 and Stx2. The black ellipse represents the carbohydrate recognition element, the biotinylated scaffold is in dark gray, and the spacers are in light gray. Figure has been adapted with permission from reference (Publisher: Wiley Interscience).[155]

A heterobivalent molecule possessing the receptors of Stx and HuSAP results in the formation of a ternary sandwich type complex (Table III, entry 19).[142] When this preorganized heterobivalent molecule is tethered to a polymer, the binding affinity for Stx increases dramatically as the HuSAP organizes the Pk saccharide for optimal binding to Stx (Table III, entry 10).[148]

B. Shiga Toxin Variants Exhibit Different Glycan Preferences

Stx2 shares 56% amino acid homology with Stx1, but is more potent than Stx1. In a murine model of disease, the lethal dose for Stx1 has been reported to be about 1.2 μg, while Stx2 is 600 times more toxic, with a lethal dose of about 2 ng.[149] Studies using a baboon model have shown that administration of purified Stx2 leads to development of HUS, while an equivalent dose of Stx1 does not.[60] Similarly, clinical epidemiological studies suggest that Stx2 is more toxic to humans.[62] In addition, emerging variants, such as Stx2b–e, which may differ from Stx2 by less than a dozen amino acids, are receiving considerable attention because some of these variants appear to be more potent than Stx2, while others are less toxic to humans.

Potency differences between the various forms of Stx appear to be associated with receptor-binding differences.[150–153] This is most clearly demonstrated for Stx2e which is toxic to pigs, but not to humans. Unlike the other forms of Stx, Stx2e uses Gb4 as a receptor instead of Gb3.[154] Recently, we have demonstrated that introduction of small changes in the structure of Pk saccharides can lead to dramatic differences in the binding affinities between Stx1 and Stx2.[155] Specifically, analogues with *N*-acetylated galactose residues of Pk trisaccharide (Fig. 4B), attached to a solid surface via biotin–streptavidin conjugation chemistry, captured Stx2 specifically, but not Stx1 (Fig. 5A). Interestingly, Pk trisaccharides, when attached to the same framework, bound very well to Stx1, but not to Stx2 (Fig. 5B).[8] It is worth mentioning that contrasting results regarding the interaction of Stx2 with Pk trisaccharide have been reported; while some studies[133] (including our own work[155]) indicate

Table III. Synthetic Ligands for Shiga Toxins

No	Compound	Assay description	Data	Ref.
1. Monovalent and bivalent systems				
1	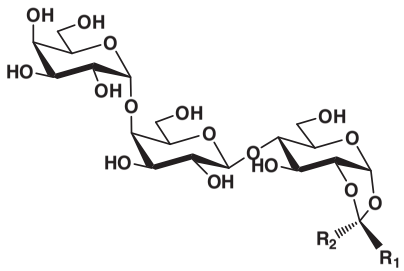 **1 : R_1 = COOH ; R_2 = CH_3** **2 : R_1 = CH_3 ; R_2 = COOH**	ELISA	Constant SAP concentration: 1: 0.56×10^{-6} M 2: no activity Varying SAP concentration: 1: 2.07×10^{-10} M, 2: no activity Inhibition of SAP binding to D-proline coated plates: 1: 1.9×10^{-3} M, 2: 1.2×10^{-3} M	292
		Mass spectrometry	1: 3.2×10^{-3} M, 2: 6.0×10^{-3} M	
2	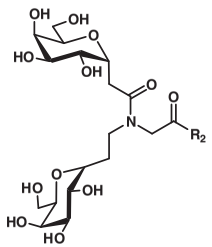 **Compounds** R_2 = 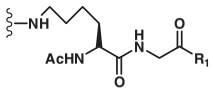 **1,2,3**  **4,5,6** 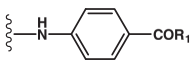 **7,8,9** **R_1 =(a) $N(CH_2CH_3)_2$, (b) $NH(CH_2)_{10}CH_3$, (c) $NH(CH_2)_{13}CH_3$**	ELISA	1,4,7: No inhibition; 2: $IC_{50} = 2.0 \times 10^{-3}$ M; 3: $IC_{50} = 0.2 \times 10^{-3}$ M; 6: $IC_{50} = 2.0 \times 10^{-3}$ M, 9: $IC_{50} = 0.2 \times 10^{-3}$ M	132

Table III. Continued

No	Compound	Assay description	Data	Ref.
3	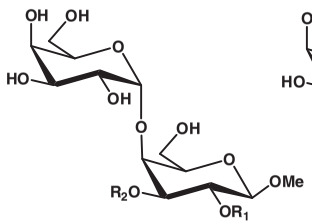 1 $R_1 = R_2 = H$ 2 $R_1 = R_2 = CH_3$ 3 $R_1 = H, R_2 = CH_3$ 4 $R_1 = CH_2CO_2H, R_2 = H$ 5 $R_1 = CH_2CH_2CO_2H, R_2 = H$ 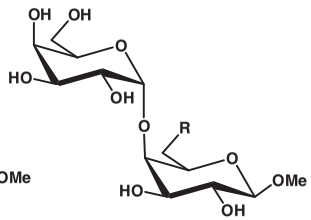 6 $R_1 = CH_2CH_2CH_2CO_2H, R_2 = H$ 7 $R_1 = CH_2CH_2OSO_3Na, R_2 = H,$ 8 $R_1 = CH_2CH_2OPO_3Na_2, R_2 = H$ 9 $R = NH_2$ 10 $R = NHAc$ 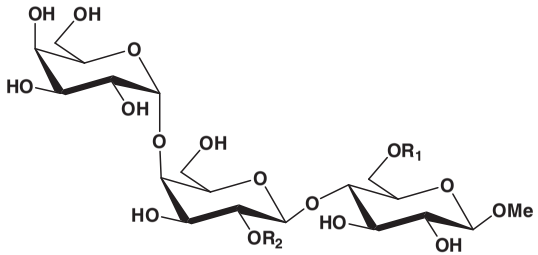 11 $R_1 = R_2 = H$ 12 $R_1 = CH_2CO_2H, R_2 = H$ 13 $R_1 = H, R_2 = CH_2CO_2H$	Solid-phase assay	1–13: $IC_{50} = 1.6–410 \times 10^{-3}$ M	135
4	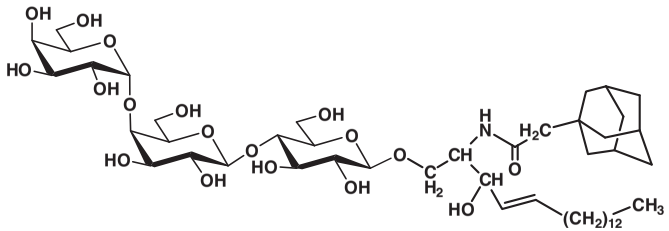	ELISA	$IC_{50} = 1 \times 10^{-6}$ M	134

5	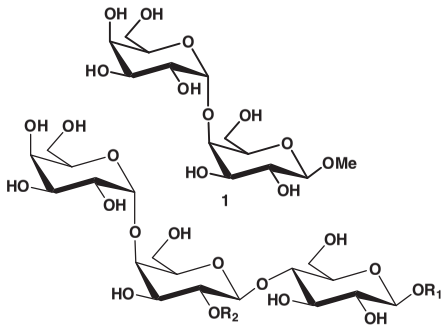	ELISA	1–9: $1/IC_{50} = 1.8–33 \times 10^4\ M^{-1}$	126

BIVALENT INHIBITORS

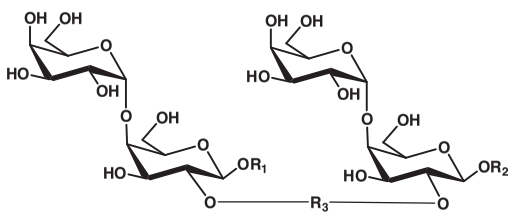

4 $R_1 = R_2 = CH3$, $R_3 = -CH_2CH_2OC(O)NHCH_2NHC(O)OCH_2CH_2-$
5 $R_1 = R_2 = CH_3$, $R_3 = -CH_2CH_2OC(O)NHCH_2CH_2CH_2NHC(O)OCH_2CH_2-$
6 $R_1 = R_2 = CH_3$, $R_3 = -C(O)NH(p\text{-}C_6H_4)NHC(O)-$
7 $R_1 = R_2 = CH_3$, $R_3 = -CH_2CH_2NH$  $NHCH_2CH_2-$

8 R_1 = (1-4)-(Me -D-Glc), $R_2 = CH_3$,
$R_3 = -CH_2CH_2OC(O)NHCH_2CH_2CH_2NHC(O)OCH_2CH_2-$
9 $R_1 = R_2$ = (1-4)-(Me -D-Glc)
$R_3 = CH_2CH_2OC(O)NHCH_2CH_2CH_2NHC(O)OCH_2CH_2-$

Table III. Continued

No	Compound	Assay description	Data	Ref.
2. Glycopolymers				
6	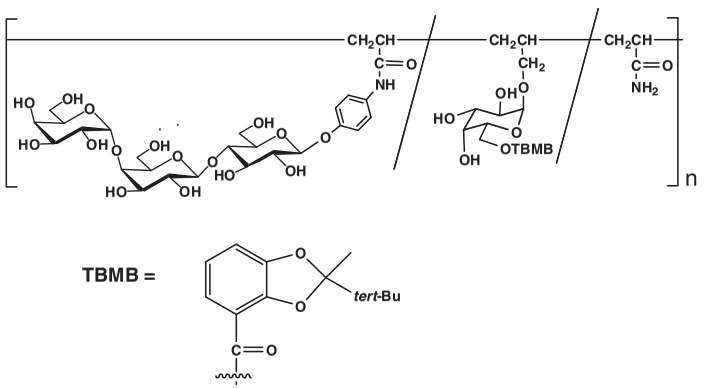	Neutralization activity against Shiga-like toxins for human ACHN cells	$K_a \sim 1.5 \times 10^5\ M^{-1}$	133
7	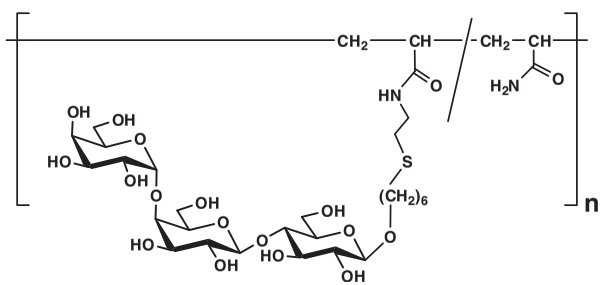	Inhibition assay on cytotoxicity of vero cells	Qualitative	293

8	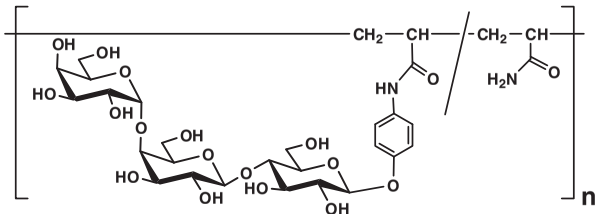	Cytotoxicity assay for HeLa cells Inhibition assay against Stx using ACHN cells	$CD_{50} = 10^{-8}$–10^{-9} M Stx1: $IC_{50} = 0.058$–0.689×10^{-6} M Stx2: $IC_{50} = 0.19$–24.3×10^{-6} M	145,294
9	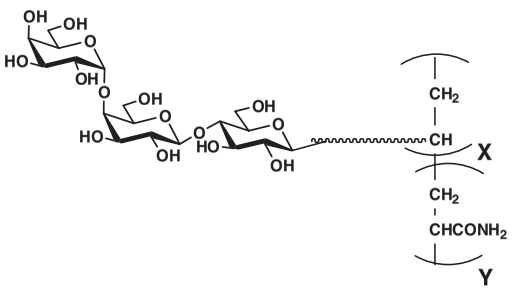	SPR Inhibition activity against Stx using vero cells	Stx1: $K_d = 0.4$ μmol/L, Stx2: $K_d = 41$ μmol/L Binding assay Stx1: $IC_{50} = 0.25$–0.33 μmol/L Stx2: $IC_{50} = 0.34$–0.6 μmol/L Cytotoxicity assay Stx1: $IC_{50} = 0.05$–0.3 μmol/L Stx2: $IC_{50} = 0.82$–26.6 μmol/L	143,295
10	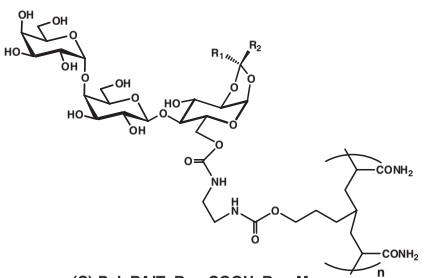 (S)-PolyBAIT R_1 = COOH, R_2 = Me (R)-PolyBAIT R_1 = Me, R_2 = COOH	ELISA (in the presence of SAP)	Stx1: (*S*)-PolyBAIT $IC_{50} = 2.7 \times 10^{-9}$ mol/L (*R*)-PolyBAIT = ND	148

Table III. Continued

No	Compound	Assay description	Data	Ref.
11	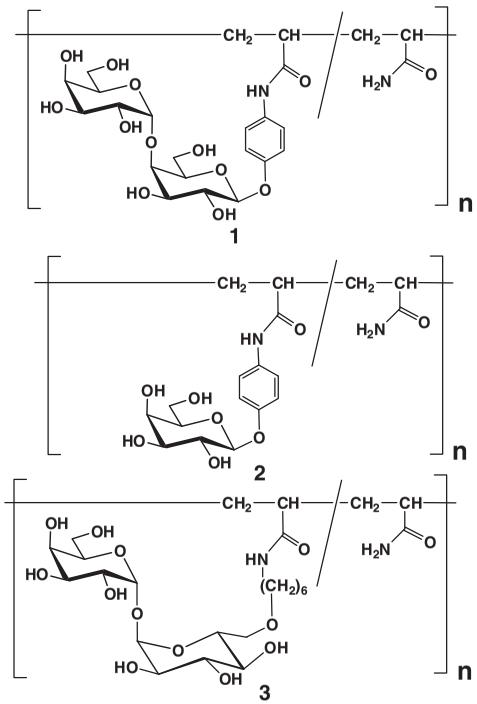	Hemagglutination inhibition assay	Stx1: (IC_{50}) 1: 4.1×10^{-5} M, 2: 1.1×10^{-3}M, 3: $>5.7 \times 10^{-2}$M Stx2: (IC_{50}) 1: 1.6×10^{-4} M, 2: $>1.1 \times 10^{-3}$ M, 3: $>5.7 \times 10^{-2}$ M	296

12	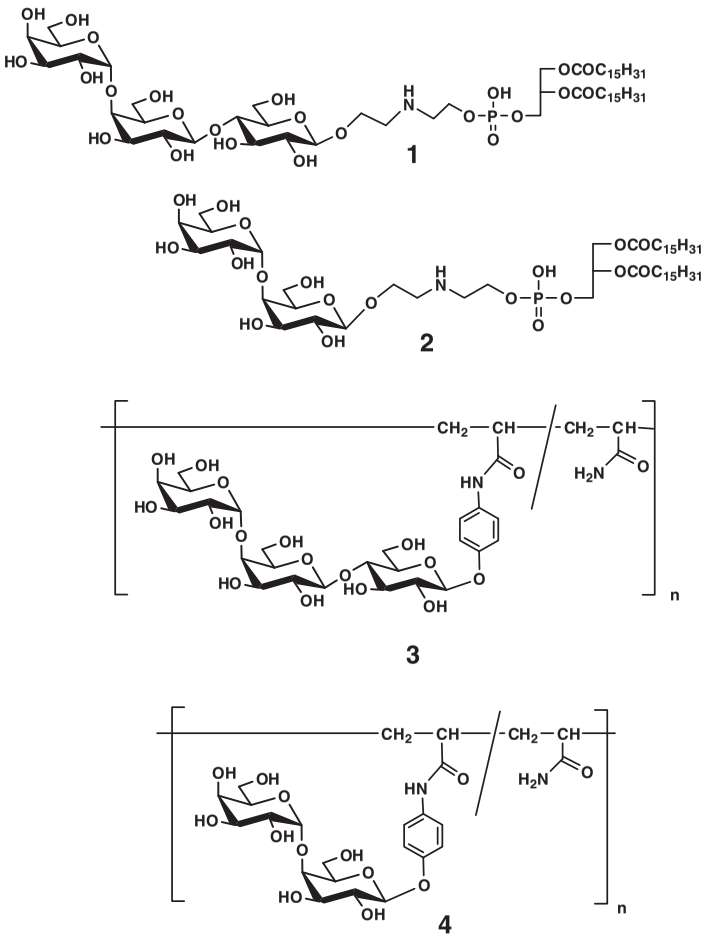	Neutralization assay	Stx1: 1: $IC_{50} = 0.5 \times 10^{-9}$ M 2: $IC_{50} = 12.54 \times 10^{-9}$ M 3: $IC_{50} = 0.58 \times 10^{-9}$ M 4: $IC_{50} = 527.3 \times 10^{-9}$ M Stx2: 1: $IC_{50} = 2.26 \times 10^{-9}$ M 2: $IC_{50} = 11.42 \times 10^{-9}$ M 3: $IC_{50} > 50 \times 10^{-6}$ M 4: $IC_{50} > 50 \times 10^{-6}$ M

Table III. Continued

No	Compound	Assay description	Data	Ref.
4. Glycodendrimers and glyconanoparticles				
13	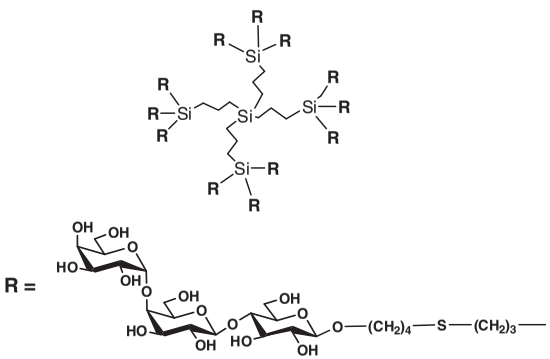	SPR	$K_d \sim 1.4\ \mu g/mL$	137
14	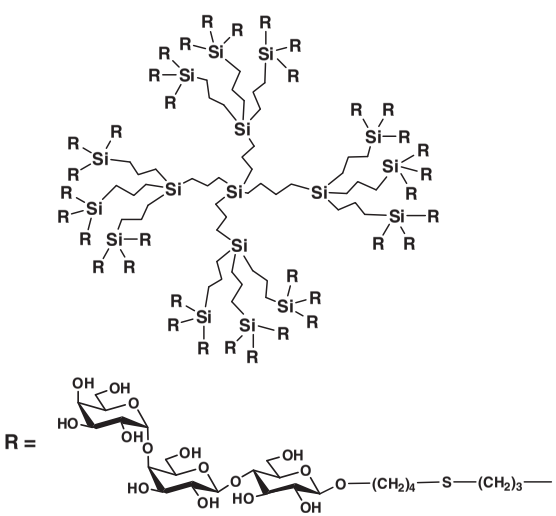	SPR	Stx1: $K_d = 0.2\ \mu mol/L$ Stx2 $K_d = 0.23\ \mu mol/L$	141

15	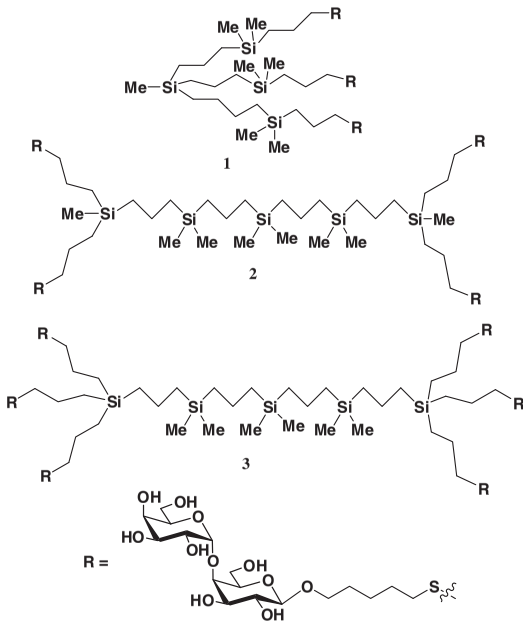	^{125}I-Stx-binding assay	Stx1: 1: $IC_{50} = 18.9 \times 10^{-6}$ M 2: $IC_{50} = 23.6 \times 10^{-6}$ M 3: $IC_{50} = 14.2 \times 10^{-6}$ M Stx2: 1: $IC_{50} = 17.8 \times 10^{-6}$ M 2: $IC_{50} = 23.6 \times 10^{-6}$ M 3: $IC_{50} = 13.6 \times 10^{-6}$ M	147

Table III. Continued

No	Compound	Assay description	Data	Ref.
16	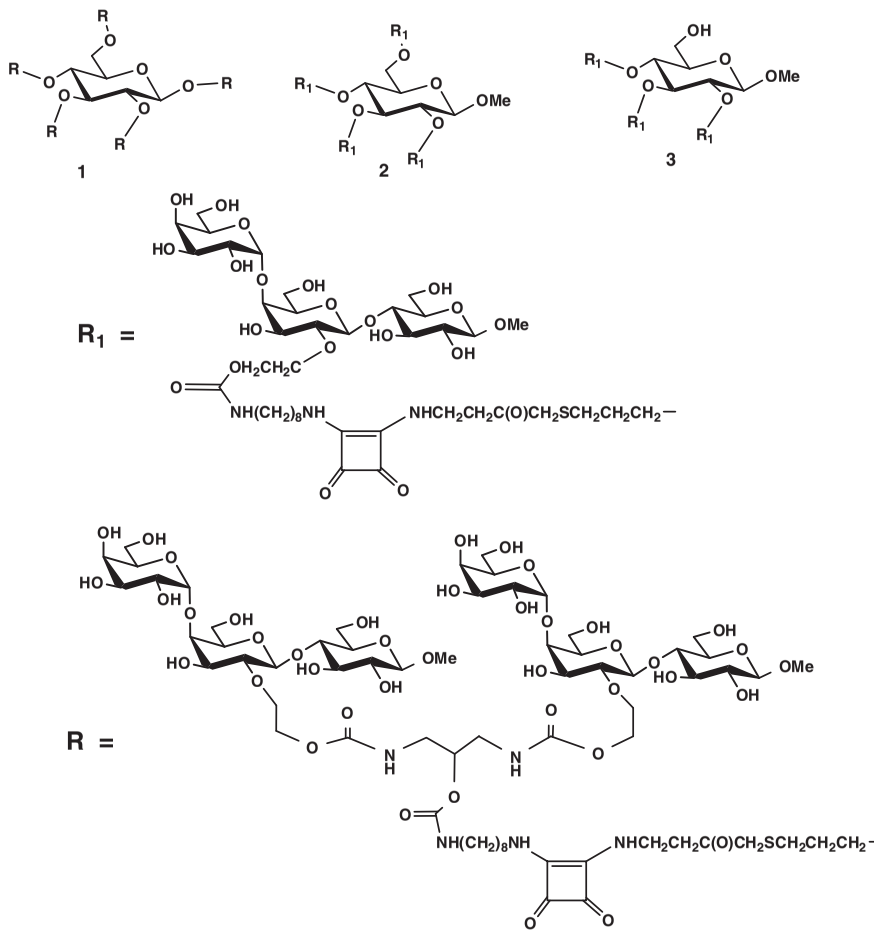	ELISA Mass spectrometry	Stx1: 1: $IC_{50} = 0.4 \times 10^{-9}$ M Stx2: 1: $IC_{50} = 6 \times 10^{-9}$ M Stx1: 3: $K_a = 1.1 \times 10^5\ M^{-1}$ Stx2: 3: $K_a = 1.5 \times 10^5\ M^{-1}$ Stx1: 2: $K_a = 1.4 \times 10^6\ M^{-1}$ Stx2: 2: $K_a = 2.6 \times 10^6\ M^{-1}$	127,144

17	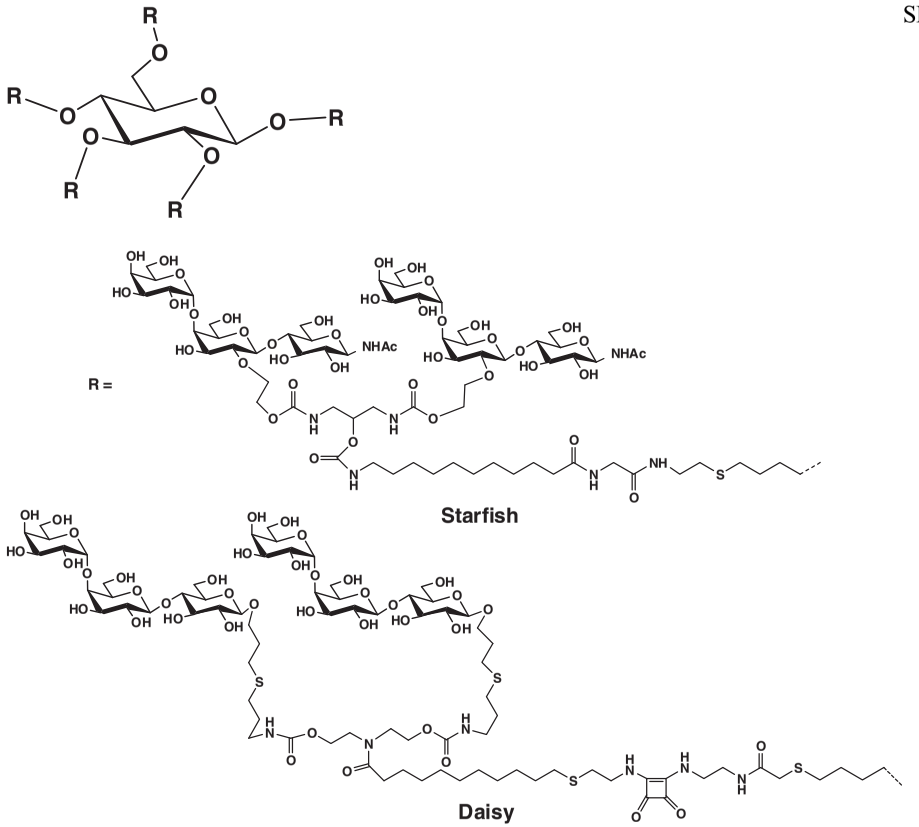	SPR Imaging	Stx1: Starfish: $IC_{50} = 1.3 \times 10^{-9}$ M Daisy: $IC_{50} = 2.6 \times 10^{-9}$ M	140

Table III. Continued

No	Compound	Assay description	Data	Ref.
18	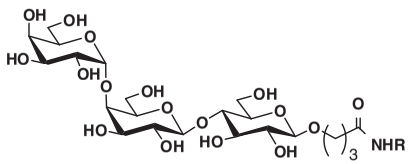 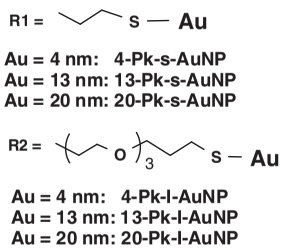	SPR competition assay	IC_{50} of nanoparticles: 4-Pk-s-AuNP: 6.54×10^{-9}; 13-Pk-s-AuNP: 3.87×10^{-10}; 20-Pk-s-AuNP: 5.29×10^{-12}; 4-Pk-I-AuNP: 8.74×10^{-11}; 13-Pk-I-AuNP: 3.06×10^{-12}; 20-Pk-I-AuNP: 1.14×10^{-12}	217
5. In vivo supramolecular template				
19	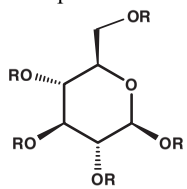 R = 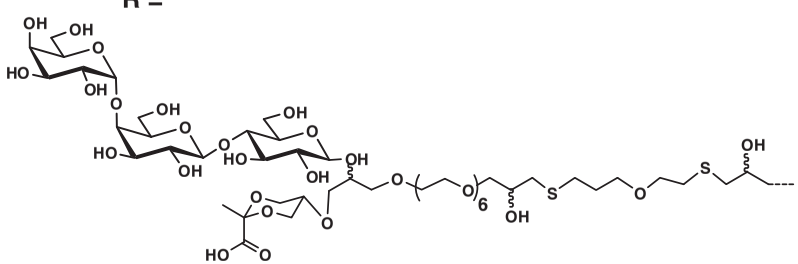	ELISA	Stx1: $IC_{50} = 140 \times 10^{-6}$ M in the absence of SAP, $IC_{50} = 4 \times 10^{-6}$ M in the presence of SAP	142

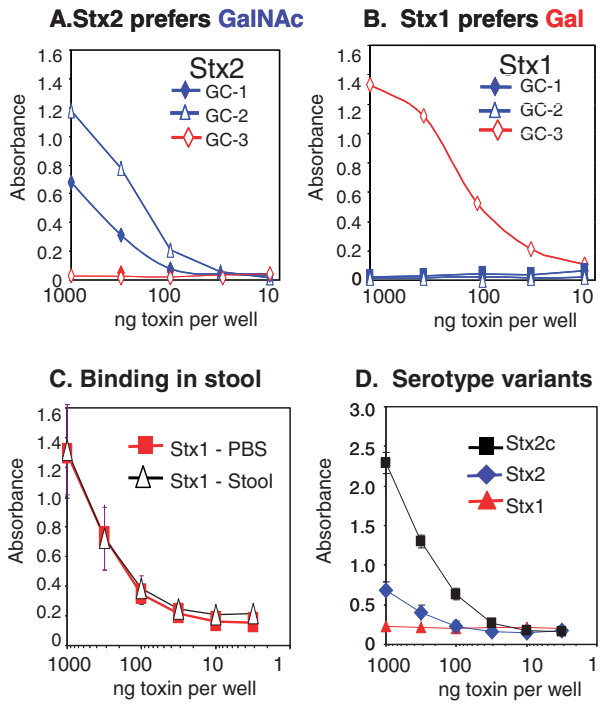

Figure 5. (**A**, **B**) Differential binding of Shiga toxin variants to synthetic glycans. (**C**) Ability of **GC-2** to capture Stx1 in human stool. (**D**) Differential binding to **GC-1**. Figure has been adapted with permission from reference (Publisher: Wiley Interscience).[218] [Color figure can be viewed in the online issue, which is available at www.interscience.wiley.com.]

that Stx2 does not bind to Pk saccharide, other studies indicate the opposite.[144] Careful examination of the contrasting reports suggests that binding of Stx2 to Pk saccharide is highly dependent on the spacer length, presentation, and assay conditions. This particular example underscores the complexity involved in understanding the "glycocode" Stx1 binds to Pk saccharides attached to a variety of platforms; however, Stx2 is more discriminatory. Nonetheless, the studies shown in Figure 5C, D are proof of principal for the use of synthetic tailored glycans to capture toxins from complex matrices and to differentiate between emerging variants.[8]

5. INFLUENZA VIRUS

Perhaps the greatest impact of the eavesdropping on the conversation between carbohydrates and pathogens has been in influenza virus research. Currently, only time separates us from the highly pathogenic strains of influenza that are expected to eventually develop a mechanism to transmit directly between humans. From a public health perspective, understanding this language has taken on a new urgency because recent reports indicate that the highly pathogenic strains of avian flu are becoming resistant to antiviral drugs.[156–159]

There are three types of influenza viruses, A, B, and C. Of these, influenza A and B are more pathogenic for humans than C, with A being the most virulent. Highly pathogenic influenza A has received the most attention. Of the ten proteins produced by influenza A,[160] the glycan-binding protein, HA, and the sialic acid cleaving enzyme, NA, mediate infection and transmission. They play a major role in determining disease outcome due to their role in mediating host immunity, transmissibility (including species and tissue specificity), and

resistance to antiviral agents. These glycoproteins exist as trimers (HA) or tetramers (NA) on the surface of the influenza virus (Fig. 6). HA mediates viral binding to the host cell and promotes viral entry. NA enzymatically removes the terminal α-linked sialic acids present on glycolipids and glycoproteins, allowing the viral progeny to escape from the surface of the infected host cell. NA also cleaves α sialic acids, present on mucins and other natural inhibitors of influenza virus, to allow the virus to move along the respiratory tract. There are 16 known HA subtypes and 9 known NA subtypes of influenza A, forming various possible combinations, such as H1N1, H3N2, H5N1, and H7N7. These subtyping schemes were originally developed using antibody panels. Antibody tests are still used to assign the H and

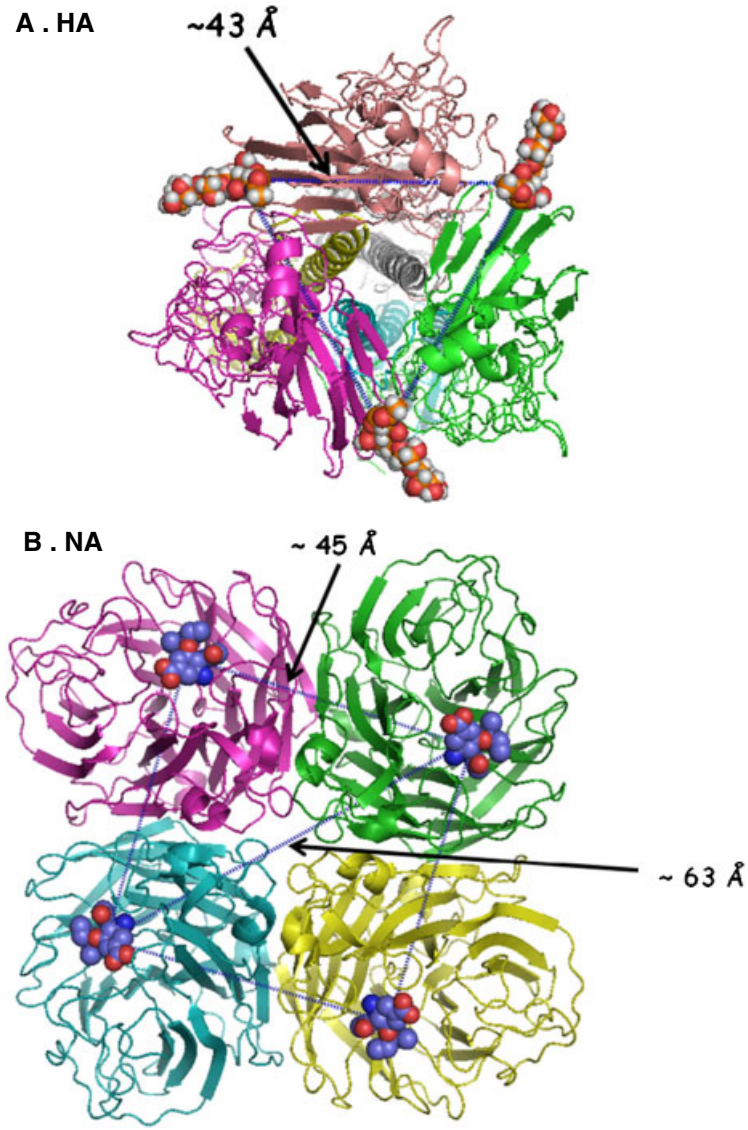

Figure 6. (**A**) Top view of ribbon diagram of HA trimer complexed with sialic acid depicting distance between the binding site of each trimer (PDB ID: 1HGD).[219] (**B**) Top view of ribbon diagram of NA tetramer complexed with sialic acid depicting distance between the binding site of each tetramer. (PDB ID : 2HU0).[220] The structures were downloaded from NCBI and the figures were generated using Pymol®.

N subtypes, but PCR techniques have been developed to detect the relevant genomic changes associated with each serotype. It is important to note that the H and N typing systems reflect viral immunogenicity, and provide useful information regarding host immunity and vaccine development. However, the HA and NA typing system itself does not provide information on glycan-binding preferences, and provides little information regarding species and cell type susceptibility, transmissibility, or pathogenic potential.

A. Host Immunity

Seasonal influenza accounts for approximately 200,000 hospitalizations and 36,000 deaths per annum in the United States. Seniors (over 65 years), children, and individuals with chronic health conditions bear the severe disease cases.[161] The impact of seasonal influenza is influenced by the presence of immune and partially immune individuals in the population. These individuals limit transmission of the virus and, ultimately, the magnitude and duration of the influenza season. The ability of immune individuals in a population to block transmission to susceptible individuals is called herd immunity. Influenza pandemics are more devastating than seasonal illness. Pandemic influenza occur when the virus acquires surface determinants, HA and NA, which are entirely new to the human population. When this happens, all individuals are fully susceptible to infection and the protective effect from herd immunity is lost. The new genes for HA and NA are acquired when human strains recombine with animal viruses, usually birds (avian influenza) or pigs (swine influenza). Pandemic outbreaks associated with H1N1 (Spanish, 1918), H2N2 (Asian, 1957), and H3N2 (Hong Kong, 1968), antigenic determinants of influenza A, were catastrophic.

B. Transmissibility and Pathogenicity

Viral transmissibility and pathogenic potential vary independently. Occasionally highly transmissible viruses are extremely virulent. The 1918 pandemic strain was notable for an especially high mortality rate, which was unusual in that young healthy adults were particularly susceptible. The high pathogenicity of the 1918 virus has been attributed to its ability to cause damage to the lungs.[163] In the spring of 2009, a new H1N1 strain with pandemic potential emerged.[164–166] This strain reportedly originated from a swine influenza source. This particular strain seems to be highly transmissible with a level 5 pandemic rating by the World Health Organization (WHO). The phase 5 level is characterized by human-to-human viral transmission in at least two countries and a strong indicator that a pandemic is imminent. At the time of writing this article, this strain remains sensitive to antiviral agents and does not seem to be as virulent as the 1918 influenza strain; however, as this viral strain continues to evolve, it might become more virulent.

In addition to possessing a new HA and NA combination, pandemic viruses must also be easily transmissible between humans. Some new viral forms, with pandemic potential, lack the ability to be easily transferred between human hosts. H5N1, also known as avian flu, primarily infects wild birds and only occasionally infects humans. Avian influenza strains are further classified as low or highly pathogenic. An emerging, highly pathogenic variant of the H5N1 avian influenza virus is raising concern. As of January 24, 2009, the WHO reports that 399 cases of H5N1 have been confirmed; of these, 252 have died, resulting in an extremely high mortality rate of 63%. However, the current variants were acquired following close contact with birds, and human-to-human transmission has not yet occurred. Newer strains are exhibiting increased drug resistance. A drug resistant form of this highly pathogenic virus would be very dangerous, if it acquired the ability to be easily transferred between human hosts.

C. Strategies to Prevent Infection

Vaccines, antivirals, diagnostics, and public health measures, such as isolation and quarantines, are the primary tools in the fight against influenza.[167] Vaccines are the mainstay against seasonal influenza; however, they cannot be developed quickly enough to prevent the first wave of infection by emerging strains. Antivirals are important for treating infected individuals and preventing death, especially in vulnerable populations, but have limited potential to prevent viral spread. Point-of-care diagnostics are probably the most important tool to prevent spread of new strains. Rapid diagnosis is important for identifying where cases of disease have emerged and which patients should be isolated. The need for diagnostics was illustrated in the recent severe acute respiratory syndrome (SARS) crisis. Lack of diagnostic tools hampered public health authorities in their efforts to rapidly identify and isolate infected patients.[168,169]

D. Influenza Virus Exhibits Different Glycan Receptor Specificities

Glycan receptor specificity has a major role in determining species and tissue specificity and transmissibility. Influenza types A, B, and C all use sialic acid as a receptor to gain cellular access (Table IB, entries 6–8); however, minute structural differences in the sialic acid residues are employed by influenza strains to achieve high selectivity, including tissue and host specificity. Efforts to identify glycan preferences of these strains have yielded considerable success, especially for type B and C.

Seminal studies conducted by Paulson and co-workers[170,171] have shown that influenza C binds specifically to a receptor, 9-*O*-acetyl-*N*-acetylneuraminic acid (9-*O*-Ac-Neu5Ac). Briefly, human asialoerythrocytes were resialylated to contain either canonical sialic acid (Neu5Ac), *N*-glycolylneuraminic acid (Neu5Gc), or 9-*O*-Ac-Neu5Ac, using purified sialyltransferases and appropriate substrates. Influenza C virus agglutinated only those cells exhibiting 9-*O*-Ac-Neu5Ac on their surface and failed to agglutinate native cells or resialylated cells containing Neu5Ac and Neu5Gc. Removal of 9-*O*-Ac-Neu5Ac from the surface resulted in loss of agglutination. These experiments identified 9-*O*-Ac-Neu5Ac as a high-affinity receptor for influenza C.

In contrast to influenza C, identification of high-affinity receptors for influenza A subtypes has been difficult, because receptor recognition by these influenza subtypes is more subtle. However, A and B can be differentiated from each other. A competitive binding assay has been used to evaluate the affinities of the receptor-binding sites of influenza A and B (Table IV).[172–176] Subtle differences at the 2 position of the lactose/lactose amine make important contributions to the binding affinities. These experiments indicate that, in addition to the Neu5Ac moiety, the composition, structure, and orientation of the internal sugars in a sialyloligosaccharide contribute significantly to the recognition event.[172,173,177–179]

Table IV. Differences in Glycan-Binding Affinities of Influenza A and B[172]

	Dissociation constant, K_d (1×10^{-3} M)	
Structure of glycans	Influenza A (A/USSR/90/77)	Influenza B (B/USSR/100/83)
Neu5Acα(2,3)Galβ(1,4)Glc	0.3	0.11
Neu5Acα(2,3)Galβ(1,4)GlcNAc	0.3	0.07
Neu5Acα(2,6)Galβ(1,4)Glc	1.5	0.3
Neu5Acα(2,6)Galβ(1,4)GlcNAc	0.1	0.3

The glycan-binding preferences of avian and human influenza A have been compared in recent studies. In general, avian influenza binds to Neu5Ac attached to the 3 position of galactose, while human influenza prefers Neu5Ac attached to the 6 position of galactose (Fig. 6). Using cultures of differentiated human airway epithelial cells, Matrosovich et al.[180] demonstrated that human influenza preferentially infected nonciliated cells bearing terminal Neu5Acα2,6Gal sugars. On the contrary, avian viruses infected ciliated cells bearing terminal Neu5Acα2,3Gal sugars. The authors conclude that infection of ciliated cells must be sub-optimal for viral replication and/or transmission in humans. These results are substantiated by observations that most human cases of avian flu have been documented to originate from infected bird contact (or in some cases, very close contact to infected humans). Avian viruses must acquire mutations in their HA proteins and switch receptor specificity from α2,3 to α2,6 linkage, in order to efficiently infect humans.[181,182]

E. Glycan Preferences of Hemagglutinin

Immunogold labeling of several influenza strains, treated with antibody to HA or NA, has revealed an estimated 50 copies of tetrameric NA and in excess of 300 copies of trimeric HA on the surface of an influenza viral particle.[183–185] Interestingly, HA is evenly distributed on the surface. In contrast, NA is present in clusters on one or more sites. The abundance of HA and NA on the viral surface makes these proteins an ideal target for anti-adhesive therapies. HA and NA (Fig. 7) recognize specific *N*-acetyl neuraminic (Neu5Ac or sialic) acid residues on termini of glycoproteins and glycolipids of the host cell.

Single crystal X-ray structures of all HAs reveal that they are very similar, with a globular domain at the apex that contains the receptor binding site, an esterase domain and a membrane proximal domain. Each HA monomer has one carbohydrate-binding site and binds to a single *N*-acetyl neuraminic acid with millimolar affinity. Three structural elements, namely the 130 loop, the 220 loop, and the 190-helix make up the relatively shallow binding pocket. The amino acids in these structural elements, the 134–138 (130 loop), 221–228 (220 loop), and 188–190 (190 α-helix) of HA1 (the *C*-terminus parent HA0) are generally conserved among all HAs with some differences in the amino acids. Changes in one or more amino acids at the receptor-binding site of HA lead to significant differences in glycan-binding affinities. Efforts to characterize minute differences in the glycan structures that specifically bind to different HA variants have used various techniques, including glycan microarray analysis, X-ray crystal structures, and biochemical analysis.[41,42,179,186–189] The glycans from the glycan microarray, developed by the Consortium for Functional Glycomics, possess Neu5Ac in a variety of linkages that include α2,3, α2,6, and α2–8 linkages. A simple

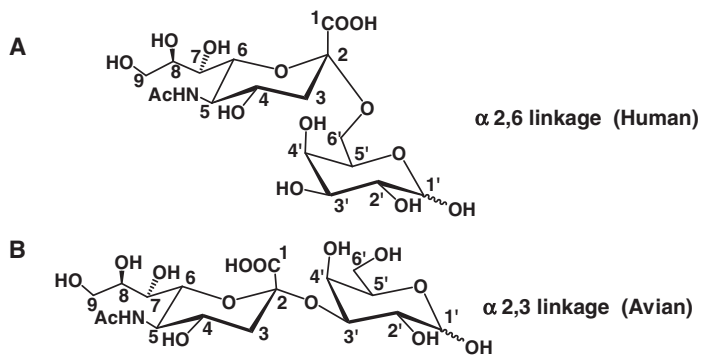

Figure 7. Structures of α 2,6 and α 2,3 galactose linked sialic acids that show preference to human and avian influenza virus, respectively.

sandwich immunoassay using recombinant HAs and fluorescent reporter antibodies were used to assess binding. Not all human HAs have identical preferences. Some H3 HAs bind to α2,3- and α2,6-linked sialosides, but no clear correlation with the inner sugar residues were observed. Two avian HAs, H5 (A/Vietnam/1203/2004) and H3 (A/Duck/Ukraine/1/1963), exhibited preferences to α2,3 sialosides, and a more detailed analysis revealed that the H5 binds to fucosylated glycans while H3 does not. Insights into the molecular details of binding were determined in a comparative study by Stevens et al.,[186] who demonstrated that a single amino acid mutation can lead to different HA binding preference. Specifically, a single amino acid residue change at position 225 from Asp (A/South Carolina/1/1918) to Gly (A/New York/1/1918) switched the HA preference from exclusively α2,6-linked sialosides to mixed specificity for both α2,6 and α2,3-linked sialosides. HA (A/New York/1/1918) was also bound to sulfated glycans. The smaller size of Gly225 is thought to allow the glycan to orient, so that the negatively charged sulfate group on the GlcNAc of Neu5Acα2,6Galβ1,4GlcNAc can form favorable hydrogen bonds with Lys222; thus, as the binding pocket opens up, the glycan can bind with a different orientation.

Attempts to correlate these *in vitro* HA binding studies to *in vivo* biological function have been performed. In a ferret model, two distinct H1N1 viruses (A/New York/1/18 and A/Texas/36/1991) exhibit mixed α2,3/α2,6 receptor specificity; however, only the Texas strain transmits effectively.[181] Sasisekaran et al. used a combination of data mining from the glycan microarray studies, molecular modeling, biochemical analysis, and examination of X-ray structures to show that the differences in transmission are due to glycan presentation.[9,190] In addition to α2,6 structural requirement, "long" α2,6 glycans with an "umbrella-like" topology promote transmission, whereas "short" α2,6 glycans that adopt a "cone-like" topology hinder transmission (Fig. 8). These findings underscore the complexity involved in developing synthetic receptor mimics; in addition to the synthesis of the correct glycan, how the glycan is presented to the cognate receptor determines the binding affinities.

Unfortunately, studies examining NA binding preferences have been limited. Current glycan microarrays are comprised mainly of naturally occurring *O*-sialosides, which can be cleaved from the surface by the action of NA. Efforts to screen the microarray in the presence of NA inhibitors and/or lowering the temperature to inhibit the cleavage activity are being attempted.

Overall, the factors that mediate glycan–HA specificity beyond broad preferences of avian and human HA, preferring α 2,3 versus α 2,6 linkages, are yet to be determined. Studies on glycan–NA and glycan—virus-binding preferences are limited due to the lack of molecules that are impervious to the action of NA. Correlation of the binding preferences of sialic acids

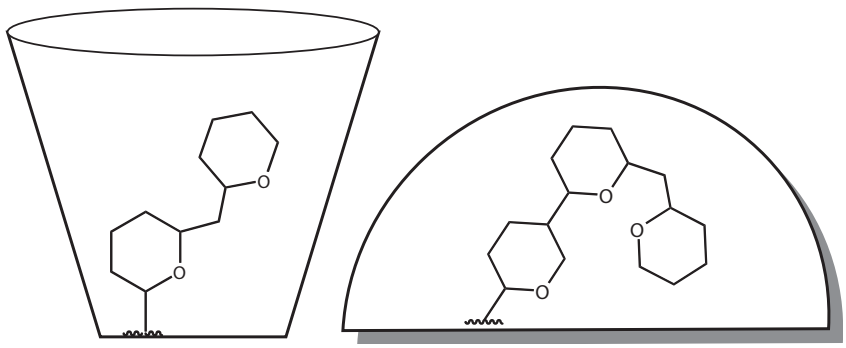

Figure 8. Topologies adopted by α 2,6 glycans. **Left**: "Short" α 2,6 glycans adopt a "cone-like" topology, which hinders facile transmission. **Right**: "Long" α 2,6 glycans adopt a "umbrella-like" topology, which seems to have a more propensity toward transmission. Figure has been adapted with permission from reference. (Publisher: Macmillan Publishers Ltd.)[218]

with HA, NA, and intact viruses is important, because it has recently been shown that certain strains of influenza exhibit decreased NA activity which might increase the virulence of these strains. Also, antivirals, such as Relenza®, which currently inhibits all influenza strains, might become ineffective against strains that exhibit decreased NA activity.

F. High-Affinity Ligands as Antiviral Agents for Influenza Virus

Several antiviral agents have been developed for treatment of influenza. The first antiviral, Amantadine®, targets the viral protein, M2, an ion channel which is required for viral uncoating. Recent efforts to inhibit the action of NA have achieved considerable success (Fig. 9) and resulted in commercial antivirals, including Relenza® (Zanamivir), which is an inhaled medication, and Tamiflu® (Oseltamivir phosphate), which can be taken orally.[156–159] These molecules resemble the transition state of the cleavage reaction of NA and bind effectively to the pathogen, but are not released from the enzyme. The molecules inhibit the action of all NAs, despite distinct differences in the structure of different NAs. Viral isolates with resistance to Tamiflu® have developed. The resistant mutants have changes in a key amino acid, Glu276, present at the active site.[159] Thus, development of additional glycan receptor mimics remains an important area of research (Tables V and VI).

The rational design and development of synthetic high-affinity ligands for influenza viruses have focused on two areas, small molecule inhibitors and multivalent displays of sialic acids that could act as competitive inhibitors. Both HA and NA are being targeted. The small molecule inhibitors include *N*-, *C*- or *S*-linked sialic acids that are impervious to the action of viral NA.[191–195] Wong et al. recently demonstrated that a fluorinated sialic acid derivative inhibits the activity of HA and NA.[196,197]

Compared to the monomeric small molecule inhibitors, multivalent displays of sialic acid exhibit increased neutralization because of their ability to engage multiple binding sites on the virus and their ability to target both glycoproteins. As in the case of Stxs, optimally tailored sialosides have been demonstrated to inhibit the virus better than random polymers. Examples include bi,[198] tri,[199] tetra,[200] or polyvalent[201] displays with sialic acid derivatives. As the number of sialic acid residues increases, the binding affinity increases. In addition to density, binding is highly dependent on the architecture of the display. Whitesides et al.[202–204]

A. Tamiflu®

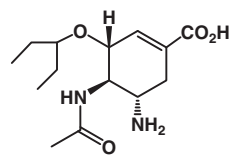

B. Relenza®

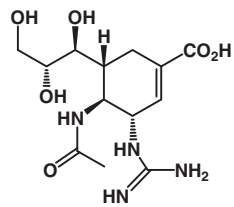

Figure 9. Structures of influenza inhibitors (**A**) Tamiflu® (Oseltamivir), the orally available NA inhibitor. (**B**) Relenza® (Zanamivir), the inhaled NA inhibitor.

Table V. High Affinity Ligands for Hemagglutinin and Intact Influenza Virus

No	Compound	Assay description	Data	Ref.
1. Monomeric systems				
1	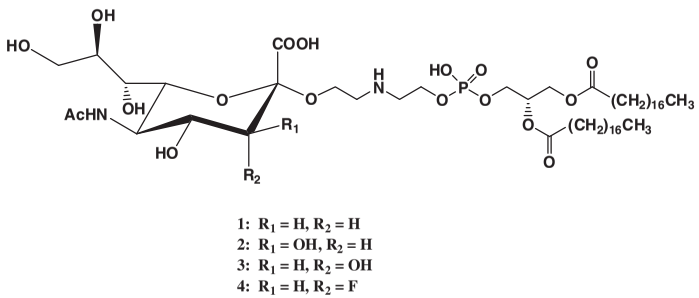	Hemagglutination inhibition assay	Human influenza virus H3N2 (A/Aichi/2/68): 1: $IC_{50} = 62.5 \times 10^{-6}$ M 2: $IC_{50} = 41.7 \times 10^{-6}$ M 3: $IC_{50} = 52.1 \times 10^{-6}$ M 4: $IC_{50} = 31.3 \times 10^{-6}$ M	196
2	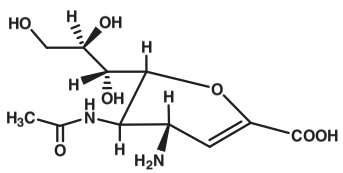	HAI activity assay	Influenza virus A (X-31): $K_i^{NA} = 50 \times 10^{-9}$ M, $K_d^{HA} 50 \times 10^{-3}$ M	297
2. Glycopolymers and glycodendrimers				
3	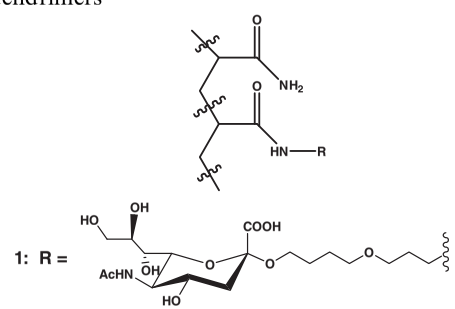	Hemagglutination inhibition assay	Influenza virus A (X-31): 1: $K_i^{HAI} = 300 \times 10^{-9}$ M 2: $K_i^{HAI} = 4 \times 10^{-9}$ M	202

4	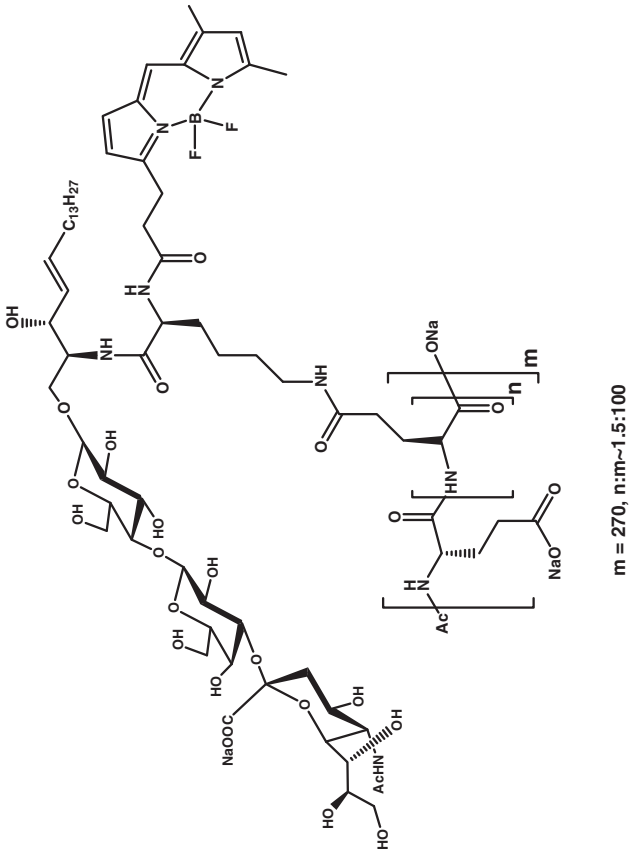 m = 270, n:m~1.5:100	ELISA	Influenza virus H1N1 (A/PR/8/34): $IC_{50} = 1.9 \times 10^{-12}$ M [298]

Table V. Continued

No	Compound	Assay description	Data	Ref.
5	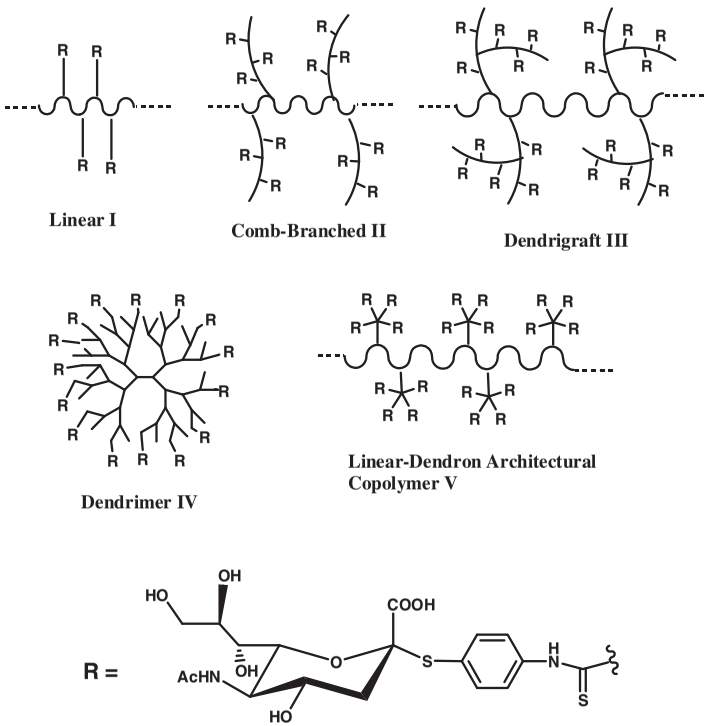	Hemagglutination inhibition assay	Fold increase in the inhibition of cRBC agglutination of influenza A H2N2 (A/AA/6/60) when compared with monomeric sialic acid: Linear polyacrylamide polymers = 64–128 fold, Spheroidal dendrimers = 32-fold, Linear dendron = 1,000-fold, Comb branched, dendrigraft = 50,000-fold	201

299

6

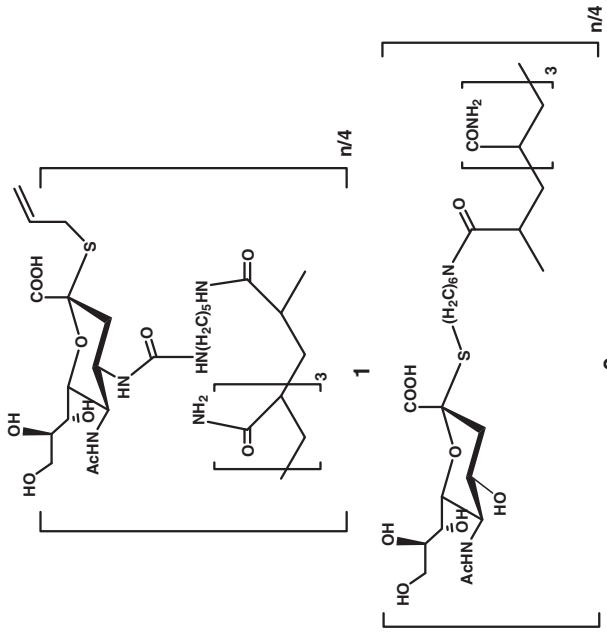

Hemagglutinin inhibition assay

Influenza virus X-31:
1: $K_i = 0.97x\ 10^{-6}$ M,
2: $K_i = 2.93 \times 10^{-6}$ M,
Influenza virus (A/Tokyo):
1: $K_i < 0.48 \times 10^{-6}$ M,
2: $K_i = 3.9 \times 10^{-6}$ M,
Influenza virus (G70C):
1: $K_i = 2.93 \times 10^{-6}$ M
2: $K_i < 0.48 \times 10^{-6}$ M

Table V. Continued

No	Compound	Assay description	Data	Ref.
7	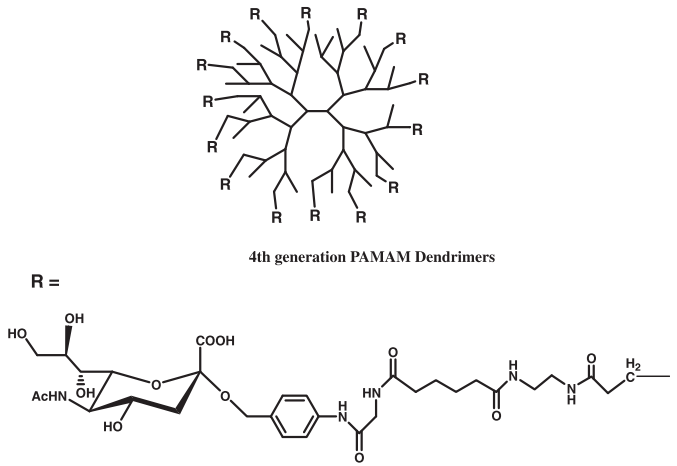	ELISA	Influenza virus (A/NIB/44/90M): $K_d = 0.001–0.1 \times 10^{-6}$ M	300
8	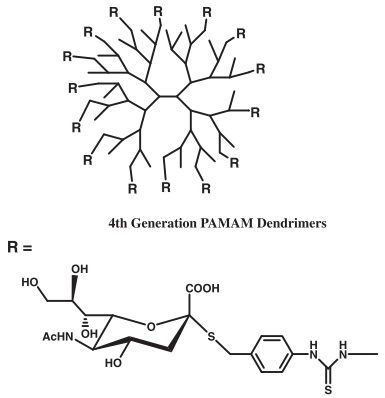	Hemagglutination inhibition assay	Fold increase in the inhibition of agglutination when compared with monomeric sialic acid: Influenza virus A H3N2 (X-31; A/Hk/8/68): 51–170 fold, Influenza virus A H1N1 strains: (A/PR/834; A/Weiss/43; A/NWS/33; A/WS/33): 32–43 fold	301

9	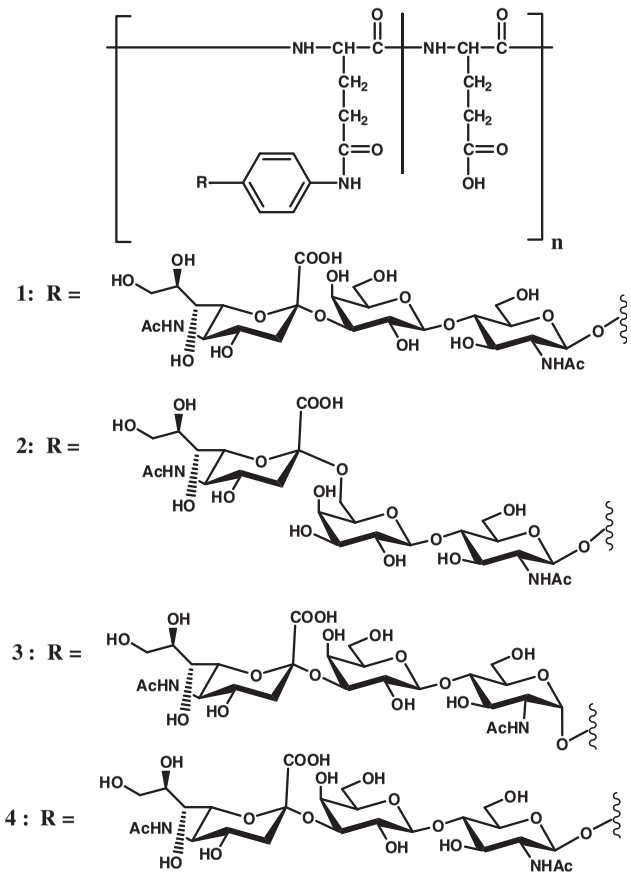	Neutralization assays	Influenza virus strains (B/Gifu/2/73; A/PR/8/34; A/Memphis/1/71; B/Lee/40; B/Gifu/2/73): $IC_{50} = 2–1{,}000 \times 10^{-6}$ M

Table V. Continued

No	Compound	Assay description	Data	Ref.
10	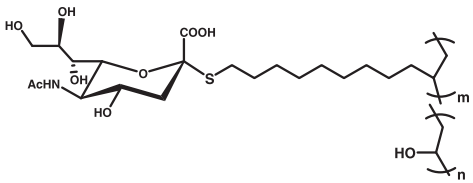	Inhibition assay	Influenza virus H3N2 (A/Memphis/1/71): $IC_{50} = 2.5 \times 10^{-3}$ M Influenza virus H1N1 (A/PR/8/34): $IC_{50} = 10 \times 10^{-3}$ M	303
11	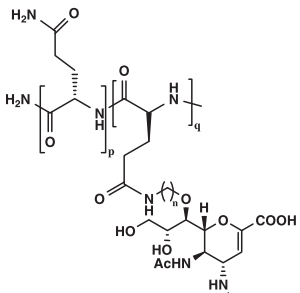 3: n = 2, p/q = 10:1 4: n = 2, p/q = 3:1 5: n = 5, p/q = 10:1 6: n = 10, p/q = 10:1 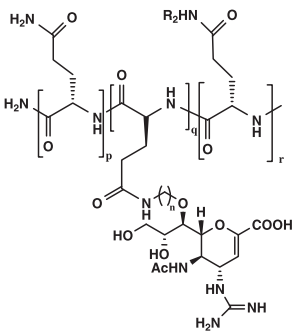 7: n = 2, R_2 = n-C_5H_{11}, p/q/r = 7:1:4 8: n = 2, R_2 = Bn, p/q/r = 7:1:4 9: n = 5, R_2 = n-C_5H_{11}, p/q/r = 8:1:2 10: n = 5, R_2 = Bn, p/q/r = 8:1:2	Sialidase inhibitory assay Plaque reduction assay	Influenza virus H1N1 (A/PR/8/34): $IC_{50} = 22–585 \times 10^{-9}$ M Influenza virus (A/Yamagata/32/89): $IC_{50} = 0.028–5.9 \times 10^{-9}$ M	304

12	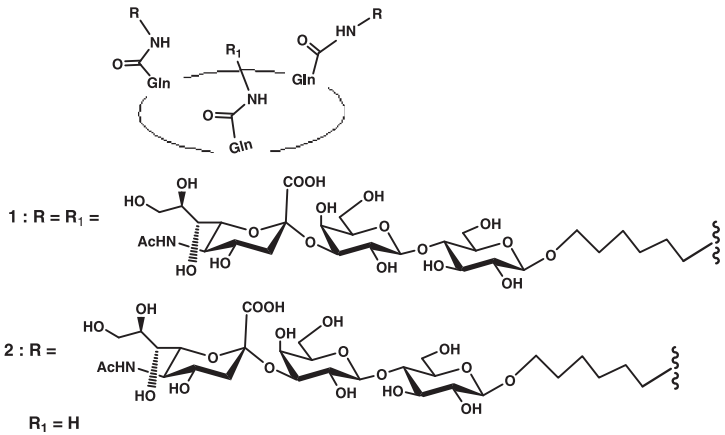	SPR	Influenza virus H1N1 (A/PR/8/34): 1: $K_d = 0.63 \times 10^{-3}$ M 2: $K_d = 1.6 \times 10^{-3}$ M	199
13	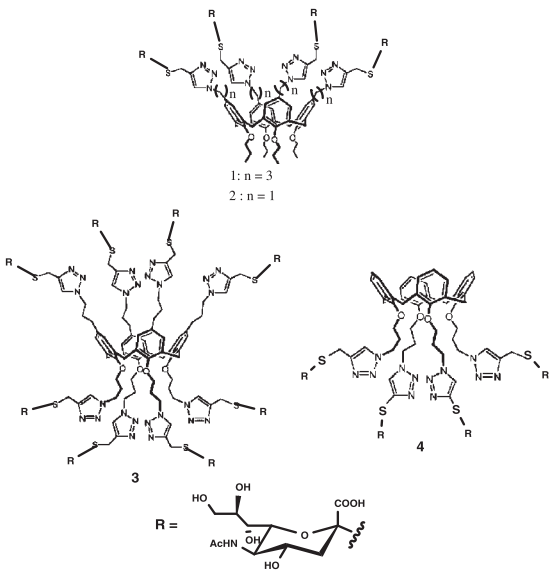	Hemagglutination inhibition assay	Influenza virus A H3N2: 1: HI activity $= 0.37 \times 10^{-3}$ M, 2: HI activity $> 50 \times 10^{-3}$ M, 3: HI activity $= 0.30 \times 10^{-3}$ M, 4: HI activity $= 0.37 \times 10^{-3}$ M	305

Table VI. High Affinity Ligands for Influenza Virus Neuraminidase

No	Compound	Assay description	Data	Ref.
1	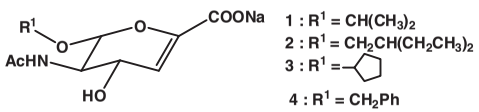	Fluorometric assay	Influenza virus neuraminidase N9: 1: $K_i = 1 \times 10^{-6}$ M 2: $K_i = 1 \times 10^{-6}$ M 3: $K_i = 1 \times 10^{-6}$ M 4: $K_i = 2.5 \times 10^{-5}$ M Influenza virus neuraminidase N2: 1: $K_i = 1 \times 10^{-6}$ M 2: $K_i = 1 \times 10^{-6}$ M 3: $K_i = 1 \times 10^{-6}$ M 4: $K_i = 2.5 \times 10^{-4}$ M	306
2	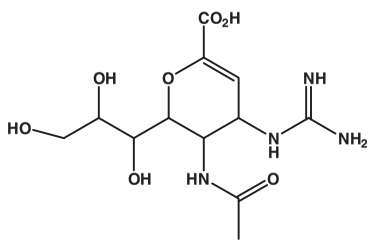 1: Zanamivir, GG167 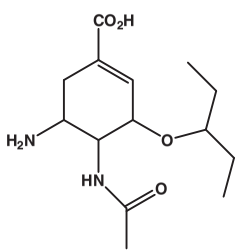 2: GS4071	Inhibition assay	Influenza virus H1N1 (B/Hong Kong/5/72-A/WS/33): 1: $IC_{50} = 1.7–0.7 \times 10^{-9}$ M 2: $IC_{50} = 0.8–1.0 \times 10^{-9}$ M	307

3	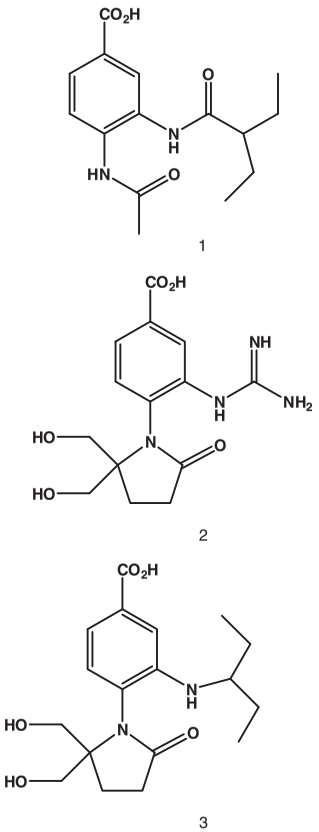	Influenza virus (B/lee/40–A/tern/Australia/G70C/75): 1: $IC_{50} = >667–26 \times 10^{-6}$ M 2: $IC_{50} = 8–5 \times 10^{-6}$ M 3: $IC_{50} = 224 \times 10^{-6}$ M–48×10^{-9} M	308

Table VI. Continued

No	Compound	Assay description	Data	Ref.
4	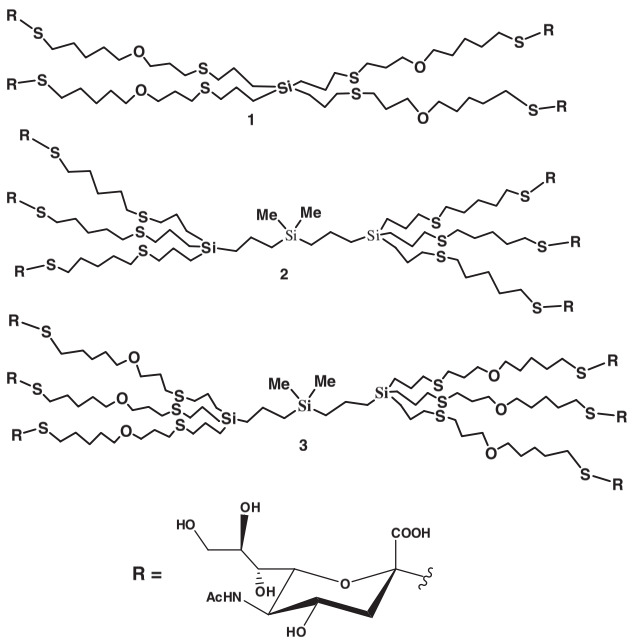	Inhibition assay against influenza virus NA	Influenza virus H3N2 (A/Memphis/1/71): 1: $IC_{50} = 5.0 \times 10^{-3}$ M 2: $IC_{50} = 5.0 \times 10^{-3}$ M 3: $IC_{50} = 1.25 \times 10^{-3}$ M Influenza virus H1N1 (A/PR/8/34): 1: $IC_{50} = 5.0 \times 10^{-3}$ M 2: $IC_{50} = 5.0 \times 10^{-3}$ M 3: $IC_{50} = 5.0 \times 10^{-3}$ M	309

and Baker et al.[201] have demonstrated that effective inhibition of the virus using polymeric systems is highly dependent on structure, density, and spacer lengths.

6. PRACTICAL APPLICATIONS OF GLYCANS

While the interactions between glycans and infectious agents can be challenging to study, once the glycan receptor is identified, further development into a therapeutic is extremely promising, as this class of compounds offers a suitable alternative to antibiotics or antivirals. Indeed, Nature uses this approach; soluble glycans, such as human milk oligosaccharides and mucins, capture and aid in removal of microbes.[205–209] Glycan-based drugs act as competitive inhibitors for the cellular receptor, arresting and eliminating the microbe in a no-kill manner.[210] Microbes may be less prone to develop resistance to this class of molecules, because in many cases glycan binding plays an intrinsic part in its pathogenic strategy. While the amino acid sequence of the carbohydrate-binding sites can change, function must be preserved; consequently, carbohydrate-based drugs may suffer less from phenotypic and genotypic drifts than vaccine and monoclonal antibody-based therapies. Currently, there are only a handful of glycan-based therapeutics approved by the FDA; however, several anti-infectives for a variety of infectious diseases are being developed.[211]

Glycans receptor mimics could be developed as capture ligands in diagnostics, and are not expected to be plagued by some of the problems associated with antibody-based diagnostics.[212] Often, it is not possible to distinguish between closely related toxins or microbes with very different pathogenic potential using polyclonal antisera, and a single amino acid change can compromise monoclonal antibody binding. As presented earlier, Stx variants, Stx1 and Stx2, share 56% amino acid identity, but differ in potency by 100- to 1,000-fold, and the difference in potency is likely due to binding differences.[61] While monoclonal antibodies can distinguish between the toxins, single amino acid mutations could alter monoclonal antibody recognition and thus eliminate detection. However, mutations that alter receptor recognition would always be accompanied by a change in potency. Thus, diagnostics based on glycan recognition are intimately tied to the biology of the toxin or pathogen, and are less susceptible to antigenic variation.[23,155] An added advantage of glycans is their extended shelf life, eliminating the need for refrigeration or freezing, which is attractive for low resource settings. Thus, understanding the "glycocode" and the subsequent development of glycan-based diagnostics and therapeutics offers distinct advantages over existing approaches.

7. CONCLUSIONS AND FUTURE DIRECTIONS

Glycans have an important but poorly understood role in regulating cellular processes and maintaining human health. They hold enormous promise for future biomedical advancements, as recent examples have shown the ability of synthetic glycans to mediate regeneration of nerve cells.[213] We have only begun to decipher the "glycocode" and the implications toward different disease states. The study of glycolipids and glycoproteins targeted by microbial pathogens provides an important research tool to investigate the basic biology of cell-surface glycans. Toxins/pathogens bind to different glycans and are also mutating constantly, leading to a large pool of variants with different glycan-binding preferences and affinities resulting in different pathogenic potential. Understanding the *in vitro* interaction of toxins and pathogens with glycans and correlating the *in vitro* binding to *in vivo* biological function

can lead to development of important therapeutics and diagnostics, and, in addition, may provide the Rosetta stone to deciphering the language of glycans.

ACKNOWLEDGMENTS

Financial support for this work was provided by NSF (CAREER CHE-0845005, S. S. I.), the UC Nanotechnology Institute (A. A. W. and S. S. I.), and NIAID (U01-AI075498 A. A. W. and S. S. I.).

REFERENCES

1. Varki A, Lowe JB. Essentials of glycobiology. In: Varki A, Cummings RD, Esko JD, Freeze HH, Stanley P, Bertozzi CR, Hart GW, Etzler ME, editors. Chapter 1, historical background and overview. 2nd ed. Plainview, NY: Cold Spring Harbor Laboratory Press; 2008.
2. Bertozzi CR, Kiessling LL. Chemical glycobiology. Science 2001;291:2357–2364.
3. Paulson JC, Blixt O, Collins BE. Sweet spots in functional glycomics. Nat Chem Biol 2006;2: 238–248.
4. Podbilewicz B. Sweet control of cell migration, cytokinesis and organogenesis. Nat Cell Biol 2004;6:9–11.
5. Ohtsubo K, Marth JD. Glycosylation in cellular mechanisms of health and disease. Cell 2006;126:855–867.
6. Raman R, Raguram S, Venkataraman G, Paulson JC, Sasisekharan R. Glycomics: An integrated systems approach to structure-function relationships of glycans. Nat Methods 2005;2:817–824.
7. Weiss AA, Iyer SS. Glycomics aims to interpret the third molecular language of cells. Microbe 2007;2:489–497.
8. Kircheis R, Vondru P, Nechansky A, Ohler R, Loibner H, Himmler G, Mudde GC. SialylTn-mAb17-1A carbohydrate-protein conjugate vaccine: Effect of coupling density and presentation of SialylTn. Bioconjug Chem 2005;16:1519–1528.
9. Chandrasekaran A, Srinivasan A, Raman R, Viswanathan K, Raguram S, Tumpey TM, Sasisekharan V, Sasisekharan R. Glycan topology determines human adaptation of avian H5N1 virus hemagglutinin. Nat Biotechnol 2008;26:107–113.
10. Dhayal M, Ratner DM. XPS and SPR analysis of glycoarray surface density. Langmuir 2009;25:2181–2187.
11. Lewallen DM, Siler D, Iyer SS. Factors affecting protein-glycan specificity: Effect of spacers and incubation time. ChemBioChem 2009;10:1486–1489.
12. Lis H, Sharon N. Protein glycosylation—structural and functional—aspects. Eur J Biochem 1993;218:1–27.
13. Davis BG. The controlled glycosylation of a protein with a bivalent glycan: Towards a new class of glycoconjugates, glycodendriproteins. Chem Commun (Camb) 2001;351–352.
14. Davis BG, Lloyd RC, Jones JB. Controlled site-selective protein glycosylation for precise glycan structure-catalytic activity relationships. Bioorg Med Chem 2000;8:1527–1535.
15. Gamblin DP, Scanlan EM, Davis BG. Glycoprotein synthesis: An update. Chem Rev 2009;109:131–163.
16. Davis BG. Synthesis of glycoproteins. Chem Rev 2002;102:579–602.
17. Ornitz DM, Herr AB, Nilsson M, Westman J, Svahn CM, Waksman G. FGF binding and FGF receptor activation by synthetic heparan-derived di- and trisaccharides. Science 1995;268:432–436.

18. Pye DA, Vives RR, Turnbull JE, Hyde P, Gallagher JT. Heparan sulfate oligosaccharides require 6-O-sulfation for promotion of basic fibroblast growth factor mitogenic activity. J Biol Chem 1998;273:22936–22942.
19. Kariya Y, Kyogashima M, Suzuki K, Isomura T, Sakamoto T, Horie K, Ishihara M, Takano R, Kamei K, Hara S. Preparation of completely 6-O-desulfated heparin and its ability to enhance activity of basic fibroblast growth factor. J Biol Chem 2000;275: 25949–25958.
20. Hakomori S. Glycosylation defining cancer malignancy: New wine in an old bottle. Proc Natl Acad Sci USA 2002;99:10231–10233.
21. Wang D. Carbohydrate microarrays. Proteomics 2003;3:2167–2175.
22. Blixt O, Head S, Mondala T, Scanlan C, Huflejt ME, Alvarez R, Bryan MC, Fazio F, Calarese D, Stevens J, Razi N, Stevens DJ, Skehel JJ, van Die I, Burton DR, Wilson IA, Cummings R, Bovin N, Wong CH, Paulson JC. Printed covalent glycan array for ligand profiling of diverse glycan binding proteins. Proc Natl Acad Sci USA 2004;101:17033–17038.
23. Disney MD, Seeberger PH. The use of carbohydrate microarrays to study carbohydrate-cell interactions and to detect pathogens. Chem Biol 2004;11:1701–1707.
24. Feizi T, Chai W. Oligosaccharide microarrays to decipher the glyco code. Nat Rev Mol Cell Biol 2004;5:582–588.
25. Lee MR, Shin I. Fabrication of chemical microarrays by efficient immobilization of hydrazide-linked substances on epoxide-coated glass surfaces. Angew Chem Int Ed Engl 2005;44:2881–2884.
26. de Paz JL, Spillmann D, Seeberger PH. Microarrays of heparin oligosaccharides obtained by nitrous acid depolymerization of isolated heparin. Chem Commun (Camb) 2006; 3116–3118.
27. Zhi ZL, Powell AK, Turnbull JE. Fabrication of carbohydrate microarrays on gold surfaces: Direct attachment of nonderivatized oligosaccharides to hydrazide-modified self-assembled monolayers. Anal Chem 2006;78:4786–4793.
28. Park S, Lee MR, Shin I. Fabrication of carbohydrate chips and their use to probe protein-carbohydrate interactions. Nat Protoc 2007;2:2747–2758.
29. Uttamchandani M, Neo JL, Ong BN, Moochhala S. Applications of microarrays in pathogen detection and biodefence. Trends Biotechnol 2009;27:53–61.
30. Wong EY, Diamond SL. Advancing microarray assembly with acoustic dispensing technology. Anal Chem 2009;81:509–514.
31. Hsu KL, Mahal LK. A lectin microarray approach for the rapid analysis of bacterial glycans. Nat Protoc 2006;1:543–549.
32. Hsu KL, Pilobello KT, Mahal LK. Analyzing the dynamic bacterial glycome with a lectin microarray approach. Nat Chem Biol 2006;2:153–157.
33. Pilobello KT, Slawek DE, Mahal LK. A ratiometric lectin microarray approach to analysis of the dynamic mammalian glycome. Proc Natl Acad Sci USA 2007;104:11534–11539.
34. Byres E, Paton AW, Paton JC, Lofling JC, Smith DF, Wilce MC, Talbot UM, Chong DC, Yu H, Huang S, Chen X, Varki NM, Varki A, Rossjohn J, Beddoe T. Incorporation of a non-human glycan mediates human susceptibility to a bacterial toxin. Nature 2008;456:648–652.
35. Dube DH, Bertozzi CR. Metabolic oligosaccharide engineering as a tool for glycobiology. Curr Opin Chem Biol 2003;7:616–625.
36. Luchansky SJ, Argade S, Hayes BK, Bertozzi CR. Metabolic functionalization of recombinant glycoproteins. Biochemistry 2004;43:12358–12366.
37. Prescher JA, Dube DH, Bertozzi CR. Chemical remodelling of cell surfaces in living animals. Nature 2004;430:873–877.
38. Laughlin ST, Agard NJ, Baskin JM, Carrico IS, Chang PV, Ganguli AS, Hangauer MJ, Lo A, Prescher JA, Bertozzi CR. Metabolic labeling of glycans with azido sugars for visualization and glycoproteomics. Methods Enzymol 2006;415:230–250.

39. Prescher JA, Bertozzi CR. Chemical technologies for probing glycans. Cell 2006;126:851–854.
40. Saxon E, Bertozzi CR. Cell surface engineering by a modified Staudinger reaction. Science 2000;287:2007–2010.
41. Stevens J, Blixt O, Glaser L, Taubenberger JK, Palese P, Paulson JC, Wilson IA. Glycan microarray analysis of the hemagglutinins from modern and pandemic influenza viruses reveals different receptor specificities. J Mol Biol 2006;355:1143–1155.
42. Stevens J, Blixt O, Paulson JC, Wilson IA. Glycan microarray technologies: Tools to survey host specificity of influenza viruses. Nat Rev Microbiol 2006;4:857–864.
43. Gildersleeve J, Roach TA, Li Z, Gildersleeve JC. Supplier-dependent antiglycan monoclonal antibody specificities: Comment on "high-throughput carbohydrate microarray profiling of 27 antibodies demonstrates widespread specificity problems." Glycobiology 2008;18:746.
44. Manimala JC, Li Z, Jain A, VedBrat S, Gildersleeve JC. Carbohydrate array analysis of anti-Tn antibodies and lectins reveals unexpected specificities: Implications for diagnostic and vaccine development. Chembiochem 2005;6:2229–2241.
45. Manimala JC, Roach TA, Li Z, Gildersleeve JC. High-throughput carbohydrate microarray analysis of 24 lectins. Angew Chem Int Ed Engl 2006;45:3607–3610.
46. Manimala JC, Roach TA, Li Z, Gildersleeve JC. High-throughput carbohydrate microarray profiling of 27 antibodies demonstrates widespread specificity problems. Glycobiology 2007;17:C17–C23.
47. Feizi T, Fazio F, Chai W, Wong CH. Carbohydrate microarrays—A new set of technologies at the frontiers of glycomics. Curr Opin Struct Biol 2003;13:637–645.
48. Hirabayashi J. Oligosaccharide microarrays for glycomics. Trends Biotechnol 2003;21: 141–143. Discussion 143.
49. Ratner DM, Adams EW, Disney MD, Seeberger PH. Tools for glycomics: Mapping interactions of carbohydrates in biological systems. Chembiochem 2004;5:1375–1383.
50. Ratner DM, Seeberger PH. Carbohydrate microarrays as tools in HIV glycobiology. Curr Pharm Des 2007;13:173–183.
51. Horlacher T, Seeberger PH. Carbohydrate arrays as tools for research and diagnostics. Chem Soc Rev 2008;37:1414–1422.
52. Rogers GN, Pritchett TJ, Lane JL, Paulson JC. Differential sensitivity of human, avian, and equine influenza A viruses to a glycoprotein inhibitor of infection: Selection of receptor specific variants. Virology 1983;131:394–408.
53. Rogers GN, D'Souza BL. Receptor binding properties of human and animal H1 influenza virus isolates. Virology 1989;173:317–322.
54. Eisen MB, Sabesan S, Skehel JJ, Wiley DC. Binding of the influenza A virus to cell-surface receptors: Structures of five hemagglutinin-sialyloligosaccharide complexes determined by X-ray crystallography. Virology 1997;232:19–31.
55. Matrosovich M, Tuzikov A, Bovin N, Gambaryan A, Klimov A, Castrucci MR, Donatelli I, Kawaoka Y. Early alterations of the receptor-binding properties of H1, H2, and H3 avian influenza virus hemagglutinins after their introduction into mammals. J Virol 2000;74: 8502–8512.
56. Ha Y, Stevens DJ, Skehel JJ, Wiley DC. X-ray structures of H5 avian and H9 swine influenza virus hemagglutinins bound to avian and human receptor analogs. Proc Natl Acad Sci USA 2001;98:11181–11186.
57. Rummel A, Eichner T, Weil T, Karnath T, Gutcaits A, Mahrhold S, Sandhoff K, Proia RL, Acharya KR, Bigalke H, Binz T. Identification of the protein receptor binding site of botulinum neurotoxins B and G proves the double-receptor concept. Proc Natl Acad Sci USA 2007;104: 359–364.
58. Baldwin MR, Kim JJ, Barbieri JT. Botulinum neurotoxin B-host receptor recognition: It takes two receptors to tango. Nat Struct Mol Biol 2007;14:9–10.

59. Rossetto O, Montecucco C. Peculiar binding of botulinum neurotoxins. ACS Chem Biol 2007;2:96–98.
60. Siegler RL, Obrig TG, Pysher TJ, Tesh VL, Denkers ND, Taylor FB. Response to Shiga toxin 1 and 2 in a baboon model of hemolytic uremic syndrome. Pediatr Nephrol 2003;18:92–96.
61. Rutjes NW, Binnington BA, Smith CR, Maloney MD, Lingwood CA. Differential tissue targeting and pathogenesis of verotoxins 1 and 2 in the mouse animal model. Kidney Int 2002;62:832–845.
62. Boerlin P, McEwen SA, Boerlin-Petzold F, Wilson JB, Johnson RP, Gyles CL. Associations between virulence factors of Shiga toxin-producing *Escherichia coli* and disease in humans. J Clin Microbiol 1999;37:497–503.
63. Haataja S, Tikkanen K, Nilsson U, Magnusson G, Karlsson KA, Finne J. Oligosaccharide-receptor interaction of the Gal alpha 1–4 Gal binding adhesin of *Streptococcus suis*. Combining site architecture and characterization of two variant adhesin specificities. J Biol Chem 1994;269:27466–27472.
64. Palmacci ER, Hewitt MC, Seeberger PH. "Cap-Tag"—Novel methods for the rapid purification of oligosaccharides prepared by automated solid-phase synthesis. Angew Chem Int Ed Engl 2001;40:4433–4437.
65. Hewitt MC, Snyder DA, Seeberger PH. Rapid synthesis of a glycosylphosphatidylinositol-based malaria vaccine using automated solid-phase oligosaccharide synthesis. J Am Chem Soc 2002;124:13434–13436.
66. Jenkins KE, Higson AP, Seeberger PH, Caruthers MH. Solid-phase synthesis and biochemical studies of O-boranophosphopeptides and O-dithiophosphopeptides. J Am Chem Soc 2002;124: 6584–6593.
67. Melean LG, Love KR, Seeberger PH. Toward the automated solid-phase synthesis of oligoglucosamines: Systematic evaluation of glycosyl phosphate and glycosyl trichloroacetimidate building blocks. Carbohydr Res 2002;337:1893–1916.
68. Plante OJ, Seeberger PH. Recent advances in automated solid-phase carbohydrate synthesis: From screening to vaccines. Curr Opin Drug Discov Devel 2003;6:521–525.
69. Ratner DM, Swanson ER, Seeberger PH. Automated synthesis of a protected N-linked glycoprotein core pentasaccharide. Org Lett 2003;5:4717–4720.
70. Seeberger PH. Automated carbohydrate synthesis to drive chemical glycomics. Chem Commun (Camb) 2003:1115–1121.
71. Holemann A, Seeberger PH. Carbohydrate diversity: Synthesis of glycoconjugates and complex carbohydrates. Curr Opin Biotechnol 2004;15:615–622.
72. Loening NM, Kanemitsu T, Seeberger PH, Griffin RG. Solid-phase synthesis and 1H and 13C high-resolution magic angle spinning NMR of 13C-labeled resin-bound saccharides. Magn Reson Chem 2004;42:453–458.
73. Routenberg Love K, Seeberger PH. Automated solid-phase synthesis of protected tumor-associated antigen and blood group determinant oligosaccharides. Angew Chem Int Ed Engl 2004;43:602–605.
74. Seeberger PH, Werz DB. Automated synthesis of oligosaccharides as a basis for drug discovery. Nat Rev Drug Discov 2005;4:751–763.
75. Coullerez G, Seeberger PH, Textor M. Merging organic and polymer chemistries to create glycomaterials for glycomics applications. Macromol Biosci 2006;6:634–647.
76. Carrel FR, Geyer K, Codee JD, Seeberger PH. Oligosaccharide synthesis in microreactors. Org Lett 2007;9:2285–2288.
77. Carrel FR, Seeberger PH. Cap-and-tag solid phase oligosaccharide synthesis. J Org Chem 2008;73:2058–2065.
78. Codee JD, Krock L, Castagner B, Seeberger PH. Automated solid-phase synthesis of protected oligosaccharides containing beta-mannosidic linkages. Chemistry: An European Journal 2008;14: 3987–3994.

79. Seeberger PH. Automated oligosaccharide synthesis. Chem Soc Rev 2008;37:19–28.
80. Burkhart F, Zhang Z, Wacowich-Sgarbi S, Wong CH. Synthesis of the globo H hexasaccharide using the programmable reactivity-based one-pot strategy. Angew Chem Int Ed Engl 2001;40:1274–1277.
81. Mong KK, Wong CH. Reactivity-based one-pot synthesis of a Lewis Y carbohydrate hapten: A colon-rectal cancer antigen determinant. Angew Chem Int Ed Engl 2002;41: 4087–4090.
82. Franke D, Machajewski T, Hsu CC, Wong CH. One-pot synthesis of L-fructose using coupled multienzyme systems based on rhamnulose-1-phosphate aldolase. J Org Chem 2003;68:6828–6831.
83. Mong TK, Huang CY, Wong CH. A new reactivity-based one-pot synthesis of N-acetyl-lactosamine oligomers. J Org Chem 2003;68:2135–2142.
84. Mong TK, Lee HK, Duron SG, Wong CH. Reactivity-based one-pot total synthesis of fucose GM1 oligosaccharide: A sialylated antigenic epitope of small-cell lung cancer. Proc Natl Acad Sci USA 2003;100:797–802.
85. Ritter TK, Mong KK, Liu H, Nakatani T, Wong CH. A programmable one-pot oligosaccharide synthesis for diversifying the sugar domains of natural products: A case study of vancomycin. Angew Chem Int Ed Engl 2003;42:4657–4660.
86. Duron SG, Polat T, Wong CH. N-(Phenylthio)-epsilon-caprolactam: A new promoter for the activation of thioglycosides. Org Lett 2004;6:839–841.
87. Lee HK, Scanlan CN, Huang CY, Chang AY, Calarese DA, Dwek RA, Rudd PM, Burton DR, Wilson IA, Wong CH. Reactivity-based one-pot synthesis of oligomannoses: Defining antigens recognized by 2G12, a broadly neutralizing anti-HIV-1 antibody. Angew Chem Int Ed Engl 2004;43:1000–1003.
88. Huang KT, Wu BC, Lin CC, Luo SC, Chen C, Wong CH. Multi-enzyme one-pot strategy for the synthesis of sialyl Lewis X-containing PSGL-1 glycopeptide. Carbohydr Res 2006;341:2151–2155.
89. Lee JC, Greenberg WA, Wong CH. Programmable reactivity-based one-pot oligosaccharide synthesis. Nat Protoc 2006;1:3143–3152.
90. Lee JC, Wu CY, Apon JV, Siuzdak G, Wong CH. Reactivity-based one-pot synthesis of the tumor-associated antigen N3 minor octasaccharide for the development of a photocleavable DIOS-MS sugar array. Angew Chem Int Ed Engl 2006;45:2753–2757.
91. Thayer DA, Wong CH. Vancomycin analogues containing monosaccharides exhibit improved antibiotic activity: A combined one-pot enzymatic glycosylation and chemical diversification strategy. Chemistry: An Asian Journal 2006;1:445–452.
92. Polat T, Wong CH. Anomeric reactivity-based one-pot synthesis of heparin-like oligosaccharides. J Am Chem Soc 2007;129:12795–12800.
93. Sugiyama M, Hong Z, Liang PH, Dean SM, Whalen LJ, Greenberg WA, Wong CH. D-Fructose-6-phosphate aldolase-catalyzed one-pot synthesis of iminocyclitols. J Am Chem Soc 2007;129:14811–14817.
94. Chen Y, Janczuk A, Chen X, Wang J, Ksebati M, Wang PG. Expeditious syntheses of two carbohydrate-linked cisplatin analogs. Carbohydr Res 2002;337:1043–1046.
95. Shao J, Zhang J, Kowal P, Wang PG. Donor substrate regeneration for efficient synthesis of globotetraose and isoglobotetraose. Appl Environ Microbiol 2002;68:5634–5640.
96. Zhang J, Kowal P, Fang J, Andreana P, Wang PG. Efficient chemoenzymatic synthesis of globotriose and its derivatives with a recombinant alpha-(1→4)-galactosyltransferase. Carbohydr Res 2002;337:969–976.
97. Shao J, Zhang J, Kowal P, Lu Y, Wang PG. Efficient synthesis of globoside and isogloboside tetrasaccharides by using beta(1→3) N-acetylgalactosaminyltransferase/UDP-N-acetylglucosamine C4 epimerase fusion protein. Chem Commun (Camb) 2003;1422–1423.

98. Cheng H, Cao X, Xian M, Fang L, Cai TB, Ji JJ, Tunac JB, Sun D, Wang PG. Synthesis and enzyme-specific activation of carbohydrate-geldanamycin conjugates with potent anticancer activity. J Med Chem 2005;48:645–652.
99. Ryu K, Lin S, Shao J, Song J, Chen M, Wang W, Li H, Yi W, Wang PG. Synthesis of complex carbohydrates and glyconjugates: Enzymatic synthesis of globotetraose using alpha-1,3-N-acetylgalactosaminyltransferase LgtD from Haemophilus infuenzae strain Rd. Methods Mol Biol 2005;310:93–105.
100. Huang GL, Mei XY, Zhang HC, Wang PG. Chemo-enzymatic synthesis of tetra-N-acetyl-chitotetraosyl allosamizoline. Bioorg Med Chem Lett 2006;16:2860–2861.
101. Huang GL, Zhang DW, Zhao HJ, Zhang HC, Wang PG. Chemo-enzymatic synthesis of allyl penta-N-acetyl-chitopentaose. Bioorg Med Chem Lett 2006;16:2042–2043.
102. Yao Q, Song J, Xia C, Zhang W, Wang PG. Chemoenzymatic syntheses of iGb3 and Gb3. Org Lett 2006;8:911–914.
103. Yu H, Chokhawala HA, Huang S, Chen X. One-pot three-enzyme chemoenzymatic approach to the synthesis of sialosides containing natural and non-natural functionalities. Nat Protoc 2006;1:2485–2492.
104. Chokhawala HA, Cao H, Yu H, Chen X. Enzymatic synthesis of fluorinated mechanistic probes for sialidases and sialyltransferases. J Am Chem Soc 2007;129:10630–10631.
105. Lewis AL, Cao H, Patel SK, Diaz S, Ryan W, Carlin AF, Thon V, Lewis WG, Varki A, Chen X, Nizet V. NeuA sialic acid O-acetylesterase activity modulates O-acetylation of capsular polysaccharide in group B Streptococcus. J Biol Chem 2007;282:27562–27571.
106. Li C, Wang HY, Wang N, Fang YG, Chen X, Yu XQ. Highly regioselective enzymatic synthesis of polymerizable derivatives of methyl shikimate. Bioorg Med Chem Lett 2007;17:6687–6690.
107. Yu H, Chen X. Carbohydrate post-glycosylational modifications. Org Biomol Chem 2007;5: 865–872.
108. Cao H, Huang S, Cheng J, Li Y, Muthana S, Son B, Chen X. Chemical preparation of sialyl Lewis × using an enzymatically synthesized sialoside building block. Carbohydr Res 2008;343: 2863–2869.
109. Chokhawala HA, Huang S, Lau K, Yu H, Cheng J, Thon V, Hurtado-Ziola N, Guerrero JA, Varki A, Chen X. Combinatorial chemoenzymatic synthesis and high-throughput screening of sialosides. ACS Chem Biol 2008;3:567–576.
110. Muthana S, Yu H, Cao H, Cheng J, Chen X. Chemoenzymatic synthesis of a new class of macrocyclic oligosaccharides. J Org Chem 2009;74:2928–2936.
111. Oyelaran O, Gildersleeve JC. Glycan arrays: recent advances and future challenges. Curr Opin Chem Biol 2009;13:406–413.
112. Oyelaran O, Li Q, Farnsworth D, Gildersleeve JC. Microarrays with varying carbohydrate density reveal distinct subpopulations of serum antibodies. J Proteome Res 2009;8:3529–3538.
113. Das SK, Mallet JM, Esnault J, Driguez PA, Duchaussoy P, Sizun P, Herault JP, Herbert JM, Petitou M, Sinay P. Synthesis of conformationally locked carbohydrates: A skew-boat conformation of L-iduronic acid governs the antithrombotic activity of heparin. Angew Chem Int Ed Engl 2001;40:1670–1673.
114. Das SK, Mallet JM, Esnault J, Driguez PA, Duchaussoy P, Sizun P, Herault JP, Herbert JM, Petitou M, Sinay P. Synthesis of conformationally locked L-iduronic acid derivatives: Direct evidence for a critical role of the skew-boat 2S0 conformer in the activation of antithrombin by heparin. Chemistry: An European Journal 2001;7:4821–4834.
115. Xu D, Newhouse EI, Amaro RE, Pao HC, Cheng LS, Markwick PRL, McCammon JA, Li WW, Arzberger PW. Distinct glycan topology for avian and human sialopentasaccharide receptor analogues upon binding different hemagglutinins: A molecular dynamics perspective. J Mol Biol 2009;387:465–491.
116. Corbell JB, Lundquist JJ, Toone EJ. A comparison of biological and calorimetric analyses of multivalent glycodendrimer ligands for concanavalin A. Tetrahedron-Asymmetry 2000;11:95–111.

117. Lundquist JJ, Toone EJ. The cluster glycoside effect. Chem Rev 2002;102:555–578.
118. Tarr PI, Gordon CA, Chandler WL. Shiga-toxin-producing *Escherichia coli* and haemolytic uraemic syndrome. Lancet 2005;365:1073–1086.
119. Siegler RL. Postdiarrheal Shiga toxin-mediated hemolytic uremic syndrome. JAMA 2003;290:1379–1381.
120. Mead PS, Slutsker L, Dietz V, McCaig LF, Bresee JS, Shapiro C, Griffin PM, Tauxe RV. Food-related illness and death in the United States. Emerg Infect Dis 1999;5:607–625.
121. Wong CS, Jelacic S, Habeeb RL, Watkins SL, Tarr PI. The risk of the hemolytic-uremic syndrome after antibiotic treatment of *Escherichia coli* O157:H7 infections. N Engl J Med 2000;342:1930–1936.
122. Gamage SD, Patton AK, Hanson JF, Weiss AA. Diversity and host range of Shiga toxin-encoding phage. Infect Immun 2004;72:7131–7139.
123. Atkinson R, Johnson G, Root T, Halse T, Wroblewski D, Davies M, Byrd A, Long L, Demma L, Angulo F, Bopp C, Gerner-Smidt P, Strockbine N, Greene K, Swaminathan B, Griffin P, Schaffzin J, Goode B. Importance of culture confirmation of Shiga toxin-producing *Escherichia coli* infection as illustrated by outbreaks of gastroenteritis—New York and North Carolina, 2005. Morbidity and Mortality Weekly Report. Volume 55: CDC; 2006. pp 1042–1045.
124. Sandvig K, van Deurs B. Entry of ricin and Shiga toxin into cells: Molecular mechanisms and medical perspectives. EMBO J 2000;19:5943–5950.
125. Lingwood CA. Glycolipid receptors for verotoxin and *Helicobacter pylori*: Role in pathology. Biochim Biophys Acta 1999;1455:375–386.
126. Kitov PI, Shimizu H, Homans SW, Bundle DR. Optimization of tether length in nonglycosidically linked bivalent ligands that target sites 2 and 1 of a Shiga-like toxin. J Am Chem Soc 2003;125:3284–3294.
127. Kitov PI, Sadowska JM, Mulvey G, Armstrong GD, Ling H, Pannu NS, Read RJ, Bundle DR. Shiga-like toxins are neutralized by tailored multivalent carbohydrate ligands. Nature 2000;403:669–672.
128. Jacewicz M, Clausen H, Nudelman E, Donohue-Rolfe A, Keusch GT. Pathogenesis of shigella diarrhea. XI. Isolation of a shigella toxin-binding glycolipid from rabbit jejunum and HeLa cells and its identification as globotriaosylceramide. J Exp Med 1986;163:1391–1404.
129. Lindberg AA, Brown JE, Stromberg N, Westling-Ryd M, Schultz JE, Karlsson KA. Identification of the carbohydrate receptor for Shiga toxin produced by Shigella dysenteriae type 1. J Biol Chem 1987;262:1779–1785.
130. Lingwood CA, Law H, Richardson S, Petric M, Brunton JL, De Grandis S, Karmali M. Glycolipid binding of purified and recombinant *Escherichia coli* produced verotoxin in vitro. J Biol Chem 1987;262:8834–8839.
131. Waddell T, Head S, Petric M, Cohen A, Lingwood C. Globotriosyl ceramide is specifically recognized by the *Escherichia coli* verocytotoxin 2. Biochem Biophys Res Commun 1988;152:674–679.
132. Arya P, Kutterer KM, Qin H, Roby J, Barnes ML, Lin S, Lingwood CA, Peter MG. Alpha-galactose based neoglycopeptides. Inhibition of verotoxin binding to globotriosylceramide. Bioorg Med Chem 1999;7:2823–2833.
133. Dohi H, Nishida Y, Mizuno M, Shinkai M, Kobayashi T, Takeda T, Uzawa H, Kobayashi K. Synthesis of an artificial glycoconjugate polymer carrying Pk-antigenic trisaccharide and its potent neutralization activity against Shiga-like toxin. Bioorg Med Chem 1999;7:2053–2062.
134. Mylvaganam M, Lingwood CA. Adamantyl globotriaosyl ceramide: A monovalent soluble mimic which inhibits verotoxin binding to its glycolipid receptor. Biochem Biophys Res Commun 1999;257:391–394.

135. Kitov PI, Bundle DR. Synthesis and structure-activity relationships of di- and trisaccharide inhibitors for shiga-like toxin Type 1. J Chem Soc, Perkin Trans 2001;1:838–853.
136. Mylvaganam M, Hansen HC, Binnington B, Magnusson G, Nyholm PG, Lingwood CA. Interaction of the verotoxin 1B subunit with soluble aminodeoxy analogues of globotriaosyl ceramides. Biochem J 2002;368:769–776.
137. Nishikawa K, Matsuoka K, Kita E, Okabe N, Mizuguchi M, Hino K, Miyazawa S, Yamasaki C, Aoki J, Takashima S, Yamakawa Y, Nishijima M, Terunuma D, Kuzuhara H, Natori Y. A therapeutic agent with oriented carbohydrates for treatment of infections by Shiga toxin-producing *Escherichia coli* O157:H7. Proc Natl Acad Sci USA 2002;99:7669–7674.
138. Kitov PI, Bundle DR. On the nature of the multivalency effect: A thermodynamic model. J Am Chem Soc 2003;125:16271–16284.
139. Mulvey GL, Marcato P, Kitov PI, Sadowska J, Bundle DR, Armstrong GD. Assessment in mice of the therapeutic potential of tailored, multivalent Shiga toxin carbohydrate ligands. J Infect Dis 2003;187:640–649.
140. Kanda V, Kitov P, Bundle DR, McDermott MT. Surface plasmon resonance imaging measurements of the inhibition of Shiga-like toxin by synthetic multivalent inhibitors. Anal Chem 2005;77:7497–7504.
141. Nishikawa K, Matsuoka K, Watanabe M, Igai K, Hino K, Hatano K, Yamada A, Abe N, Terunuma D, Kuzuhara H, Natori Y. Identification of the optimal structure required for a Shiga toxin neutralizer with oriented carbohydrates to function in the circulation. J Infect Dis 2005;191:2097–2105.
142. Solomon D, Kitov PI, Paszkiewicz E, Grant GA, Sadowska JM, Bundle DR. Heterobifunctional multivalent inhibitor-adaptor mediates specific aggregation between Shiga toxin and a pentraxin. Org Lett 2005;7:4369–4372.
143. Watanabe M, Igai K, Matsuoka K, Miyagawa A, Watanabe T, Yanoshita R, Samejima Y, Terunuma D, Natori Y, Nishikawa K. Structural analysis of the interaction between Shiga toxin B subunits and linear polymers bearing clustered globotriose residues. Infect Immun 2006;74:1984–1988.
144. Kitova EN, Kitov PI, Paszkiewicz E, Kim J, Mulvey GL, Armstrong GD, Bundle DR, Klassen JS. Affinities of Shiga toxins 1 and 2 for univalent and oligovalent Pk-trisaccharide analogs measured by electrospray ionization mass spectrometry. Glycobiology 2007;17: 1127–1137.
145. Neri P, Nagano SI, Yokoyama S, Dohi H, Kobayashi K, Miura T, Inazu T, Sugiyama T, Nishida Y, Mori H. Neutralizing activity of polyvalent Gb3, Gb2 and galacto-trehalose models against Shiga toxins. Microbiol Immunol 2007;51:581–592.
146. Neri P, Tokoro S, Yokoyama S, Miura T, Murata T, Nishida Y, Kajimoto T, Tsujino S, Inazu T, Usui T, Mori H. Monovalent Gb3-/Gb2-derivatives conjugated with a phosphatidyl residue: A novel class of Shiga toxin-neutralizing agent. Biol Pharm Bull 2007;30:1697–1701.
147. Yamada A, Hatano K, Matsuoka K, Koyama T, Esumi Y, Koshino H, Hino K, Nishikawa K, Natori Y, Terunuma D. Syntheses and vero toxin-binding activities of carbosilane dendrimers periphery-functionalized with galabiose. Tetrahedron 2006;62:5074–5083.
148. Kitov PI, Mulvey GL, Griener TP, Lipinski T, Solomon D, Paszkiewicz E, Jacobson JM, Sadowska JM, Suzuki M, Yamamura K, Armstrong GD, Bundle DR. In vivo supramolecular templating enhances the activity of multivalent ligands: A potential therapeutic against the *Escherichia coli* O157 AB5 toxins. Proc Natl Acad Sci USA 2008;105:16837–16842.
149. Tesh VL, Burris JA, Owens JW, Gordon VM, Wadolkowski EA, O'Brien AD, Samuel JE. Comparison of the relative toxicities of Shiga-like toxins type I and type II for mice. Infect Immun 1993;61:3392–3402.
150. Miura Y, Sasao Y, Dohi H, Nishida Y, Kobayashi K. Self-assembled monolayers of globotriaosylceramide (Gb3) mimics: Surface-specific affinity with Shiga toxins. Anal Biochem 2002;310:27–35.

151. Kiarash A, Boyd B, Lingwood CA. Glycosphingolipid receptor function is modified by fatty acid content. Verotoxin 1 and verotoxin 2c preferentially recognize different globotriaosyl ceramide fatty acid homologues. J Biol Chem 1994;269:11138–11146.
152. Manning SD, Motiwala AS, Springman AC, Qi W, Lacher DW, Ouellette LM, Mladonicky JM, Somsel P, Rudrik JT, Dietrich SE, Zhang W, Swaminathan B, Alland D, Whittam TS. Variation in virulence among clades of *Escherichia coli* O157:H7 associated with disease outbreaks. Proc Natl Acad Sci USA 2008;105:4868–4873.
153. Persson S, Olsen KE, Ethelberg S, Scheutz F. Subtyping method for *Escherichia coli* Shiga toxin (verocytotoxin) 2 variants and correlations to clinical manifestations. J Clin Microbiol 2007;45:2020–2024.
154. Paton AW, Morona R, Paton JC. Neutralization of Shiga toxins Stx1, Stx2c, and Stx2e by recombinant bacteria expressing mimics of globotriose and globotetraose. Infect Immun 2001;69:1967–1970.
155. Kale RR, McGannon CM, Fuller-Schaefer C, Hatch DM, Flagler MJ, Gamage SD, Weiss AA, Iyer SS. Differentiation between structurally homologous Shiga 1 and Shiga 2 toxins by using synthetic glycoconjugates. Angew Chem Int Ed Engl 2008;47:1265–1268.
156. Cheung CL, Rayner JM, Smith GJ, Wang P, Naipospos TS, Zhang J, Yuen KY, Webster RG, Peiris JS, Guan Y, Chen H. Distribution of amantadine-resistant H5N1 avian influenza variants in Asia. J Infect Dis 2006;193:1626–1629.
157. Gupta RK, Nguyen-Van-Tam JS. Oseltamivir resistance in influenza A (H5N1) infection. N Engl J Med 2006;354:1423–1424.
158. He G, Qiao J, Dong C, He C, Zhao L, Tian Y. Amantadine-resistance among H5N1 avian influenza viruses isolated in Northern China. Antiviral Res 2008;77:72–76.
159. Le QM, Kiso M, Someya K, Sakai YT, Nguyen TH, Nguyen KH, Pham ND, Ngyen HH, Yamada S, Muramoto Y, Horimoto T, Takada A, Goto H, Suzuki T, Suzuki Y, Kawaoka Y. Avian flu: Isolation of drug-resistant H5N1 virus. Nature 2005;437:1108.
160. Salomon R, Webster RG. The influenza virus enigma. Cell 2009;136:402–410.
161. Carolyn B, Bridges KF, Uyeki TM, Cox NJ, Singleton JA. Recommendations and Reports, Morbidity and Mortality Weekly Report. Vol 51: CDC; 2002. pp 1–31.
162. Kilbourne ED. Influenza pandemics of the 20th century. Emerg Infect Dis 2006;12:9–14.
163. Kash JC, Tumpey TM, Proll SC, Carter V, Perwitasari O, Thomas MJ, Basler CF, Palese P, Taubenberger JK, Garcia-Sastre A, Swayne DE, Katze MG. Genomic analysis of increased host immune and cell death responses induced by 1918 influenza virus. Nature 2006;443:578–581.
164. Centers for Disease C, Prevention. Update: Infections with a swine-origin influenza A (H1N1) virus—United States and other countries, Morbidity and Mortality Weekly Report. Vol 58: CDC; 2009. pp 431–433.
165. Cohen J, Enserink M. Infectious diseases. As swine flu circles globe, scientists grapple with basic questions. Science 2009;324:572–573.
166. Butler D. Swine flu goes global. Nature 2009;458:1082–1083.
167. von Itzstein M. The war against influenza: Discovery and development of sialidase inhibitors. Nat Rev Drug Discov 2007;6:967–974.
168. Ooi PL, Lim S, Tham KW. Lessons from SARS in an age of emerging infections. Med Lav 2006;97:369–375.
169. Tan BH, Jin-Phang J, Seah SGK, Koh VWH, Lim EAS, Liaw C, Ong CEL, Chew JSW, Wang DL, Lim EP, Yap SH, Aw LT, Lim APC, Liu YC, Lee MA. Strategies adopted and lessons learnt during the severe acute respiratory syndrome crisis in Singapore. Rev Med Virol 2005;15:57–70.
170. Herrler G, Gross HJ, Imhof N, Brossmer R, Milks G, Paulson JC. A synthetic sialic acid analogue is recognized by influenza C virus as a recpetor determinant but is resistant to the receptor destroying enzyme. J Biol Chem 1992;267:12501–12505.

171. Rogers GN, Georg H, Paulson JC, Klenk HD. Influenza C virus uses 9-O-acetyl-N-acetylneuraminic acid as a high affinity receptor determinant for attachment to cells. J Biol Chem 1986;261:5947–5951.
172. Gambaryan AS, Piskarev VE, Yamskov IA, Sakharov AM, Tuzikov AB, Bovin NV, Nifant'ev NE, Matrosovich MN. Human influenza virus recognition of sialyloligosaccharides. FEBS Lett 1995;366:57–60.
173. Matrosovich MN, Gambaryan AS, Tuzikov AB, Byramova NE, Mochalova LV, Golbraikh AA, Shenderovich MD, Finne J, Bovin NV. Probing of the receptor binding sites of the H1 and H3 influenza A and influenza B virus hemagglutinins by synthetic and natural sialosides. Virology 1993;196:111–121.
174. Suzuki Y, Nakao T, Ito T, Watanabe N, Toda Y, Xu GY, Suzuki T, Kobayashi T, Kimura Y, Yamada A, Sugawara K, Nishimura H, Kitame F, Nakamura K, Deya E, Kiso M, Hasegawa A. Structural determination of gangliosides that bind to influenza A, B, and C viruses by an improved binding assay: strain-specific receptor epitopes in sialo-sugar chains. Virology 1992;189:121–131.
175. Connor RJ, Kawaoka Y, Webster RG, Paulson JC. Receptor specificity in human, avian, and equine H2 and H3 influenza virus isolates. Virology 1994;205:17–23.
176. Gambaryan AS, Matrosovich MN. A solid-phase enzyme-linked assay for influenza virus receptor-binding activity. J Virol Methods 1992;39:111–123.
177. Gambaryan A, Yamnikova S, Lvov D, Tuzikov A, Chinarev A, Pazynina G, Webster R, Matrosovich M, Bovin N. Receptor specificity of influenza viruses from birds and mammals: New data on involvement of the inner fragments of the carbohydrate chain. Virology 2005;334:276–283.
178. Gambaryan AS, Karasin AI, Tuzikov AB, Chinarev AA, Pazynina GV, Bovin NV, Matrosovich MN, Olsen CW, Klimov AI. Receptor-binding properties of swine influenza viruses isolated and propagated in MDCK cells. Virus Res 2005;114:15–22.
179. Nicholls JM, Chan RW, Russell RJ, Air GM, Peiris JS. Evolving complexities of influenza virus and its receptors. Trends Microbiol 2008;16:149–157.
180. Matrosovich MN, Matrosovich TY, Gray T, Roberts NA, Klenk HD. Human and avian influenza viruses target different cell types in cultures of human airway epithelium. Proc Natl Acad Sci USA 2004;101:4620–4624.
181. Tumpey TM, Maines TR, Van Hoeven N, Glaser L, Solorzano A, Pappas C, Cox NJ, Swayne DE, Palese P, Katz JM, Garcia-Sastre A. A two-amino acid change in the hemagglutinin of the 1918 influenza virus abolishes transmission. Science 2007;315:655–659.
182. Yamada S, Suzuki Y, Suzuki T, Le MQ, Nidom CA, Sakai-Tagawa Y, Muramoto Y, Ito M, Kiso M, Horimoto T, Shinya K, Sawada T, Kiso M, Usui T, Murata T, Lin Y, Hay A, Haire LF, Stevens DJ, Russell RJ, Gamblin SJ, Skehel JJ, Kawaoka Y. Haemagglutinin mutations responsible for the binding of H5N1 influenza A viruses to human-type receptors. Nature 2006;444:378–382.
183. Amano H, Uemoto H, Kuroda K, Hosaka Y. Immunoelectron microscopy of influenza A virus neuraminidase glycoprotein topography. J Gen Virol 1992;73:1969–1975.
184. Leser GP, Lamb RA. Influenza virus assembly and budding in raft-derived microdomains: A quantitative analysis of the surface distribution of HA, NA and M2 proteins. Virology 2005;342:215–227.
185. Murti KG, Webster RG. Distribution of hemagglutinin and neuraminidase on influenza virions as revealed by immunoelectron microscopy. Virology 1986;149:36–43.
186. Stevens J, Blixt O, Tumpey TM, Taubenberger JK, Paulson JC, Wilson IA. Structure and receptor specificity of the hemagglutinin from an H5N1 influenza virus. Science 2006;312:404–410.
187. Belser JA, Blixt O, Chen LM, Pappas C, Maines TR, Van Hoeven N, Donis R, Busch J, McBride R, Paulson JC, Katz JM, Tumpey TM. Contemporary North American influenza H7 viruses possess human receptor specificity: Implications for virus transmissibility. Proc Natl Acad Sci USA 2008;105:7558–7563.

188. Gulati U, Wu W, Gulati S, Kumari K, Waner JL, Air GM. Mismatched hemagglutinin and neuraminidase specificities in recent human H3N2 influenza viruses. Virology 2005;339: 12–20.

189. Kumari K, Gulati S, Smith DF, Gulati U, Cummings RD, Air GM. Receptor binding specificity of recent human H3N2 influenza viruses. Virol J 2007;4:42.

190. Srinivasan A, Viswanathan K, Raman R, Chandrasekaran A, Raguram S, Tumpey TM, Sasisekharan V, Sasisekharan R. Quantitative biochemical rationale for differences in transmissibility of 1918 pandemic influenza A viruses. Proc Natl Acad Sci USA 2008;105: 2800–2805.

191. Yuan X, Ress DK, Linhardt RJ. Synthesis of nor-C-linked neuraminic acid disaccharide: A versatile precursor of C-analogs of oligosialic acids and gangliosides. J Org Chem 2007;72: 3085–3088.

192. Wilson JC, Kiefel MJ, Angus DI, von Itzstein M. Investigation of the stability of thiosialosides toward hydrolysis by sialidases using NMR spectroscopy. Org Lett 1999;1: 443–446.

193. Kim JH, Huang F, Ly M, Linhardt RJ. Stereoselective synthesis of a C-linked neuraminic acid disaccharide: Potential building block for the synthesis of C-analogues of polysialic acids. J Org Chem 2008;73:9497–9500.

194. Sparks MA, Williams KW, Whitesides GM. Neuraminidase-resistant hemagglutination inhibitors: Acrylamide copolymers containing a C-glycoside of N-acetylneuraminic acid. J Med Chem 1993;36:778–783.

195. Wang Q, Wolff M, Polat T, Du Y, Linhardt RJ. Inhibition of neuraminidase with neuraminic acid C-glycosides. Bioorg Med Chem Lett 2000;10:941–944.

196. Guo CT, Sun XL, Kanie O, Shortridge KF, Suzuki T, Miyamoto D, Hidari KI, Wong CH, Suzuki Y. An O-glycoside of sialic acid derivative that inhibits both hemagglutinin and sialidase activities of influenza viruses. Glycobiology 2002;12:183–190.

197. Sun XL, Kanie Y, Guo CT, Kanie O, Suzuki Y, Wong CH. Syntheses of C-3-modified sialylglycosides as selective inhibitors of influenza hemagglutinin and neuraminidase. Eur J Org Chem 2000:2643–2653.

198. Glick GD, Toogood PL, Wiley DC, Skehel JJ, Knowles JR. Ligand recognition by influenza virus. The binding of bivalent sialosides. J Biol Chem 1991;266:23660–23669.

199. Ohta T, Miura N, Fujitani N, Nakajima F, Niikura K, Sadamoto R, Guo CT, Suzuki T, Suzuki Y, Monde K, Nishimura S. Glycotentacles: Synthesis of cyclic glycopeptides, toward a tailored blocker of influenza virus hemagglutinin. Angew Chem Int Ed Engl 2003;42: 5186–5189.

200. Inoue Y, Lee YC, Troy FA, II, editors. Sialobiology and other novel forms of glycosylation. Osaka, Japan: Gakushin Publishing Co; 1999. pp 135–143.

201. Reuter JD, Myc A, Hayes MM, Gan Z, Roy R, Qin D, Yin R, Piehler LT, Esfand R, Tomalia DA, Baker JR, Jr. Inhibition of viral adhesion and infection by sialic-acid-conjugated dendritic polymers. Bioconjug Chem 1999;10:271–278.

202. George B, Sigal MM, Dahmann G, Whitesides GM. Polyacrylamides bearing pendant R-sialoside groups strongly inhibit agglutination of erythrocytes by influenza virus: The strong inhibition reflects enhanced binding through cooperative polyvalent interactions. J Am Chem Soc 1996;118:3789–3800.

203. Lees WJ, Spaltenstein A, Kingery-Wood JE, Whitesides GM. Polyacrylamides bearing pendant alpha-sialoside groups strongly inhibit agglutination of erythrocytes by influenza A virus: Multivalency and steric stabilization of particulate biological systems. J Med Chem 1994;37:3419–3433.

204. Mammen M, Dahmann G, Whitesides GM. Effective inhibitors of hemagglutination by influenza virus synthesized from polymers having active ester groups. Insight into mechanism of inhibition. J Med Chem 1995;38:4179–4190.

205. Andersson B, Porras O, Hanson LA, Lagergard T, Svanborg-Eden C. Inhibition of attachment of Streptococcus pneumoniae and Haemophilus influenzae by human milk and receptor oligosaccharides. J Infect Dis 1986;153:232–237.
206. Newburg DS. Oligosaccharides in human milk and bacterial colonization. J Pediatr Gastroenterol Nutr 2000;30:S8–S17.
207. Martin-Sosa S, Martin MJ, Hueso P. The sialylated fraction of milk oligosaccharides is partially responsible for binding to enterotoxigenic and uropathogenic *Escherichia coli* human strains. J Nutr 2002;132:3067–3072.
208. Ruiz-Palacios GM, Cervantes LE, Ramos P, Chavez-Munguia B, Newburg DS. Campylobacter jejuni binds intestinal H(O) antigen (Fuc alpha 1, 2Gal beta 1, 4GlcNAc), and fucosyloligosaccharides of human milk inhibit its binding and infection. J Biol Chem 2003;278:14112–14120.
209. Herrera-Insua I, Gomez HF, Diaz-Gonzalez VA, Chaturvedi P, Newburg DS, Cleary TG. Human milk lipids bind Shiga toxin. Adv Exp Med Biol 2001;501:333–339.
210. Kunz C, Rudloff S, Baier W, Klein N, Strobel S. Oligosaccharides in human milk: Structural, functional, and metabolic aspects. Annu Rev Nutr 2000;20:699–722.
211. Seeberger PH, Werz DB. Synthesis and medical applications of oligosaccharides. Nature 2007;446: 1046–1051.
212. Ngundi MM, Kulagina NV, Anderson GP, Taitt CR. Nonantibody-based recognition: Alternative molecules for detection of pathogens. Expert Rev Proteomics 2006;3:511–524.
213. Kasteren SI, Campbell SJ, Serres S, Anthony DC, Sibson NR, Davis BG. Glyconanoparticles allow pre-symptomatic *in vivo* imaging of brain disease. Proc Natl Acad Sci USA 2009;106: 18–23.
214. Fraser ME, Chernaia MM, Kozlov YV, James MN. Crystal structure of the holotoxin from Shigella dysenteriae at 2.5 A resolution. Nat Struct Biol 1994;1:59–64.
215. Fraser ME, Fujinaga M, Cherney MM, Melton-Celsa AR, Twiddy EM, O'Brien AD, James MN. Structure of Shiga toxin type 2 (Stx2) from *Escherichia coli* O157:H7. J Biol Chem 2004;279:27511–27517.
216. Ling H, Boodhoo A, Hazes B, Cummings MD, Armstrong GD, Brunton JL, Read RJ. Structure of the Shiga-like toxin I B-pentamer complexed with an analogue of its receptor Gb3. Biochemistry 1998;37:1777–1788.
217. Chien YY, Jan MD, Adak AK, Tzeng HC, Lin YP, Chen YJ, Wang KT, Chen CT, Chen CC, Lin CC. Globotriose-functionalized gold nanoparticles as multivalent probes for Shiga-like toxin. Chembiochem 2008;9:1100–1109.
218. Bewley CA. Illuminating the switch in influenza viruses. Nat Biotechnol 2008;26:60–62.
219. Sauter NK, Hanson JE, Glick GD, Brown JH, Crowther RL, Park SJ, Skehel JJ, Wiley DC. Binding of influenza virus hemagglutinin to analogs of its cell-surface receptor, sialic acid: Analysis by proton nuclear magnetic resonance spectroscopy and X-ray crystallography. Biochemistry 1992;31:9609–9621.
220. Russell RJ, Haire LF, Stevens DJ, Collins PJ, Lin YP, Blackburn GM, Hay AJ, Gamblin SJ, Skehel JJ. The structure of H5N1 avian influenza neuraminidase suggests new opportunities for drug design. Nature 2006;443:45–49.
221. Merritt EA, Sarfaty S, van den Akker F, L'Hoir C, Martial JA, Hol WG. Crystal structure of cholera toxin B-pentamer bound to receptor GM1 pentasaccharide. Protein Sci 1994;3:166–175.
222. Merritt EA, Sarfaty S, Jobling MG, Chang T, Holmes RK, Hirst TR, Hol WG. Structural studies of receptor binding by cholera toxin mutants. Protein Sci 1997;6:1516–1528.
223. Merritt EA, Kuhn P, Sarfaty S, Erbe JL, Holmes RK, Hol WG. The 1.25 A resolution refinement of the cholera toxin B-pentamer: Evidence of peptide backbone strain at the receptor-binding site. J Mol Biol 1998;282:1043–1059.
224. Bernardi A, Arosio D, Potenza D, Sanchez-Medina I, Mari S, Canada FJ, Jimenez-Barbero J. Intramolecular carbohydrate-aromatic interactions and intermolecular van der Waals

interactions enhance the molecular recognition ability of GM1 glycomimetics for cholera toxin. Chemistry: An European Journal 2004;10:4395.

225. Turnbull WB, Precious BL, Homans SW. Dissecting the cholera toxin-ganglioside GM1 interaction by isothermal titration calorimetry. J Am Chem Soc 2004;126:1047–1054.
226. MacKenzie CR, Hirama T, Lee KK, Altman E, Young NM. Quantitative analysis of bacterial toxin affinity and specificity for glycolipid receptors by surface plasmon resonance. J Biol Chem 1997;272:5533–5538.
227. Sixma TK, Pronk SE, Kalk KH, van Zanten BA, Berghuis AM, Hol WG. Lactose binding to heat-labile enterotoxin revealed by X-ray crystallography. Nature 1992;355: 561–564.
228. Holmner A, Askarieh G, Okvist M, Krengel U. Blood group antigen recognition by *Escherichia coli* heat-labile enterotoxin. J Mol Biol 2007;371:754–764.
229. Stein PE, Boodhoo A, Armstrong GD, Heerze LD, Cockle SA, Klein MH, Read RJ. Structure of a pertussis toxin-sugar complex as a model for receptor binding. Nat Struct Biol 1994;1:591–596.
230. Gomez SR, Xing DK, Corbel MJ, Coote J, Parton R, Yuen CT. Development of a carbohydrate binding assay for the B-oligomer of pertussis toxin and toxoid. Anal Biochem 2006;356:244–253.
231. Lindberg AA, Brown JE, Stromberg N, Westling-Ryd M, Schultz JE, Karlsson KA. Identification of the carbohydrate receptor for Shiga toxin produced by Shigella dysenteriae type 1. J Biol Chem 1987;262:1779–1785.
232. Waddell T, Head S, Petric M, Cohen A, Lingwood C. Globotriosyl ceramide is specifically recognized by the *Escherichia coli* verocytotoxin 2. Biochem Biophys Res Commun 1988;152:674–679.
233. Gamage SD, McGannon CM, Weiss AA. *Escherichia coli* serogroup O107/O117 lipopolysaccharide binds and neutralizes Shiga toxin 2. J Bacteriol 2004;186:5506–5512.
234. Jayaraman S, Eswaramoorthy S, Kumaran D, Swaminathan S. Common binding site for disialyllactose and tri-peptide in C-fragment of tetanus neurotoxin. Proteins 2005;61: 288–295.
235. Emsley P, Fotinou C, Black I, Fairweather NF, Charles IG, Watts C, Hewitt E, Isaacs NW. The structures of the H(C) fragment of tetanus toxin with carbohydrate subunit complexes provide insight into ganglioside binding. J Biol Chem 2000;275:8889–8894.
236. Fotinou C, Emsley P, Black I, Ando H, Ishida H, Kiso M, Sinha KA, Fairweather NF, Isaacs NW. The crystal structure of tetanus toxin Hc fragment complexed with a synthetic GT1b analogue suggests cross-linking between ganglioside receptors and the toxin. J Biol Chem 2001;276:32274–32281.
237. Conway MC, Whittal RM, Baldwin MA, Burlingame AL, Balhorn R. Electrospray mass spectrometry of NeuAc oligomers associated with the C fragment of the tetanus toxin. J Am Soc Mass Spectrom 2006;17:967–976.
238. Stenmark P, Dupuy J, Imamura A, Kiso M, Stevens RC. Crystal structure of botulinum neurotoxin type A in complex with the cell surface co-receptor GT1b-insight into the toxin-neuron interaction. PLoS Pathog 2008;4:e1000129.
239. Swaminathan S, Eswaramoorthy S. Structural analysis of the catalytic and binding sites of Clostridium botulinum neurotoxin B. Nat Struct Biol 2000;7:693–699.
240. Nakamura T, Tonozuka T, Ide A, Yuzawa T, Oguma K, Nishikawa A. Sugar-binding sites of the HA1 subcomponent of *Clostridium botulinum* type C progenitor toxin. J Mol Biol 2008;376:
854–867.
241. Greco A, Ho JG, Lin SJ, Palcic MM, Rupnik M, Ng KK. Carbohydrate recognition by Clostridium difficile toxin A. Nat Struct Mol Biol 2006;13:460–461.

242. Tucker KD, Wilkins TD. Toxin A of Clostridium difficile binds to the human carbohydrate antigens I, X, and Y. Infect Immun 1991;59:73–78.

243. Swaminathan S, Furey W, Pletcher J, Sax M. Residues defining V beta specificity in staphylococcal enterotoxins. Nat Struct Biol 1995;2:680–686.

244. Chung MC, Wines BD, Baker H, Langley RJ, Baker EN, Fraser JD. The crystal structure of staphylococcal superantigen-like protein 11 in complex with sialyl Lewis X reveals the mechanism for cell binding and immune inhibition. Mol Microbiol 2007;66:1342–1355.

245. Baker HM, Basu I, Chung MC, Caradoc-Davies T, Fraser JD, Baker EN. Crystal structures of the staphylococcal toxin SSL5 in complex with sialyl Lewis X reveal a conserved binding site that shares common features with viral and bacterial sialic acid binding proteins. J Mol Biol 2007;374:1298–1308.

246. Blanchard B, Nurisso A, Hollville E, Tetaud C, Wiels J, Pokorna M, Wimmerova M, Varrot A, Imberty A. Structural basis of the preferential binding for globo-series glycosphingolipids displayed by *Pseudomonas aeruginosa* lectin I. J Mol Biol 2008;383:837–853.

247. Cioci G, Mitchell EP, Gautier C, Wimmerova M, Sudakevitz D, Perez S, Gilboa-Garber N, Imberty A. Structural basis of calcium and galactose recognition by the lectin PA-IL of *Pseudomonas aeruginosa*. FEBS Lett 2003;555:297–301.

248. Lameignere E, Malinovska L, Slavikova M, Duchaud E, Mitchell EP, Varrot A, Sedo O, Imberty A, Wimmerova M. Structural basis for mannose recognition by a lectin from opportunistic bacteria *Burkholderia cenocepacia*. Biochem J 2008;411:307–318.

249. Pokorna M, Cioci G, Perret S, Rebuffet E, Kostlanova N, Adam J, Gilboa-Garber N, Mitchell EP, Imberty A, Wimmerova M. Unusual entropy-driven affinity of *Chromobacterium violaceum* lectin CV-IIL toward fucose and mannose. Biochemistry 2006;45:7501–7510.

250. Perret S, Sabin C, Dumon C, Pokorna M, Gautier C, Galanina O, Ilia S, Bovin N, Nicaise M, Desmadril M, Gilboa-Garber N, Wimmerova M, Mitchell EP, Imberty A. Structural basis for the interaction between human milk oligosaccharides and the bacterial lectin PA-IIL of *Pseudomonas aeruginosa*. Biochem J 2005;389:325–332.

251. Mitchell E, Houles C, Sudakevitz D, Wimmerova M, Gautier C, Perez S, Wu AM, Gilboa-Garber N, Imberty A. Structural basis for oligosaccharide-mediated adhesion of *Pseudomonas aeruginosa* in the lungs of cystic fibrosis patients. Nat Struct Biol 2002;9:918–921.

252. Sudakevitz D, Kostlanova N, Blatman-Jan G, Mitchell EP, Lerrer B, Wimmerova M, Katcoff DJ, Imberty A, Gilboa-Garber N. A new *Ralstonia solanacearum* high-affinity mannose-binding lectin RS-IIL structurally resembling the *Pseudomonas aeruginosa* fucose-specific lectin PA-IIL. Mol Microbiol 2004;52:691–700.

253. Bu W, Mamedova A, Tan M, Xia M, Jiang X, Hegde RS. Structural basis for the receptor binding specificity of Norwalk virus. J Virol 2008;82:5340–5347.

254. Rydell GE, Nilsson J, Rodriguez-Diaz J, Ruvoen-Clouet N, Svensson L, Le Pendu J, Larson G. Human noroviruses recognize sialyl Lewis X neoglycoprotein. Glycobiology 2009;19:309–320.

255. Choi JM, Hutson AM, Estes MK, Prasad BV. Atomic resolution structural characterization of recognition of histo-blood group antigens by Norwalk virus. Proc Natl Acad Sci USA 2008;105:9175–9180.

256. Harrington PR, Vinje J, Moe CL, Baric RS. Norovirus capture with histo-blood group antigens reveals novel virus-ligand interactions. J Virol 2004;78:3035–3045.

257. Cao S, Lou Z, Tan M, Chen Y, Liu Y, Zhang Z, Zhang XC, Jiang X, Li X, Rao Z. Structural basis for the recognition of blood group trisaccharides by norovirus. J Virol 2007; 81:5949–5957.

258. Blanchard H, Yu X, Coulson BS, von Itzstein M. Insight into host cell carbohydrate-recognition by human and porcine rotavirus from crystal structures of the virion spike associated carbohydrate-binding domain (VP8*). J Mol Biol 2007;367:1215–1226.

259. Dormitzer PR, Sun ZY, Wagner G, Harrison SC. The rhesus rotavirus VP4 sialic acid binding domain has a galectin fold with a novel carbohydrate binding site. EMBO J 2002;21:885–897.

260. Kraschnefski MJ, Bugarcic A, Fleming FE, Yu X, von Itzstein M, Coulson BS, Blanchard H. Effects on sialic acid recognition of amino acid mutations in the carbohydrate-binding cleft of the rotavirus spike protein. Glycobiology 2009;19:194–200.
261. Fazli A, Bradley SJ, Kiefel MJ, Jolly C, Holmes IH, von Itzstein M. Synthesis and biological evaluation of sialylmimetics as rotavirus inhibitors. J Med Chem 2001;44:3292–3301.
262. Fry EE, Lea SM, Jackson T, Newman JW, Ellard FM, Blakemore WE, Abu-Ghazaleh R, Samuel A, King AM, Stuart DI. The structure and function of a foot-and-mouth disease virus-oligosaccharide receptor complex. EMBO J 1999;18:543–554.
263. Stehle T, Harrison SC. High-resolution structure of a polyomavirus VP1-oligosaccharide complex: Implications for assembly and receptor binding. EMBO J 1997;16:5139–5148.
264. Stehle T, Harrison SC. Crystal structures of murine polyomavirus in complex with straight-chain and branched-chain sialyloligosaccharide receptor fragments. Structure 1996;4:183–194.
265. Burmeister WP, Guilligay D, Cusack S, Wadell G, Arnberg N. Crystal structure of species D adenovirus fiber knobs and their sialic acid binding sites. J Virol 2004;78:7727–7736.
266. Johansson SM, Arnberg N, Elofsson M, Wadell G, Kihlberg J. Multivalent HSA conjugates of 3′-sialyllactose are potent inhibitors of adenoviral cell attachment and infection. ChemBioChem 2005;6:358–364.
267. Gunther I, Glatthaar B, Doller G, Garten W. A H1 hemagglutinin of a human influenza A virus with a carbohydrate-modulated receptor binding site and an unusual cleavage site. Virus Res 1993;27:147–160.
268. Hidari KI, Shimada S, Suzuki Y, Suzuki T. Binding kinetics of influenza viruses to sialic acid-containing carbohydrates. Glycoconj J 2007;24:583–590.
269. Gamblin SJ, Haire LF, Russell RJ, Stevens DJ, Xiao B, Ha Y, Vasisht N, Steinhauer DA, Daniels RS, Elliot A, Wiley DC, Skehel JJ. The structure and receptor binding properties of the 1918 influenza hemagglutinin. Science 2004;303:1838–1842.
270. Lin T, Wang G, Li A, Zhang Q, Wu C, Zhang R, Cai Q, Song W, Yuen KY. The hemagglutinin structure of an avian H1N1 influenza A virus. Virology 2009;392:73–81.
271. Wang Q, Tian X, Chen X, Ma J. Structural basis for receptor specificity of influenza B virus hemagglutinin. Proc Natl Acad Sci USA 2007;104:16874–16879.
272. Harms G, Reuter G, Corfield AP, Schauer R. Binding specificity of influenza C-virus to variably O-acetylated glycoconjugates and its use for histochemical detection of N-acetyl-9-O-acetylneuraminic acid in mammalian tissues. Glycoconj J 1996;13:621–630.
273. Mastromarino P, Cioe L, Rieti S, Orsi N. Role of membrane phospholipids and glycolipids in the vero cell surface receptor for rubella virus. Med Microbiol Immunol 1990;179:105–114.
274. Epand RM, Nir S, Parolin M, Flanagan TD. The role of the ganglioside GD1a as a receptor for Sendai virus. Biochemistry 1995;34:1084–1089.
275. Chiba A, Matsumura K, Yamada H, Inazu T, Shimizu T, Kusunoki S, Kanazawa I, Kobata A, Endo T. Structures of sialylated O-linked oligosaccharides of bovine peripheral nerve alpha-dystroglycan. The role of a novel O-mannosyl-type oligosaccharide in the binding of alpha-dystroglycan with laminin. J Biol Chem 1997;272:2156–2162.
276. Neu U, Woellner K, Gauglitz G, Stehle T. Structural basis of GM1 ganglioside recognition by simian virus 40. Proc Natl Acad Sci USA 2008;105:5219–5224.
277. Campanero-Rhodes MA, Smith A, Chai W, Sonnino S, Mauri L, Childs RA, Zhang Y, Ewers H, Helenius A, Imberty A, Feizi T. N-glycolyl GM1 ganglioside as a receptor for simian virus 40. J Virol 2007;81:12846–12858.
278. Qadri F, Haque A, Faruque SM, Bettelheim KA, Robins-Browne R, Albert MJ. Hemagglutinating properties of enteroaggregative *Escherichia coli*. J Clin Microbiol 1994;32:510–514.

279. Kuehn MJ, Heuser J, Normark S, Hultgren SJ. P pili in uropathogenic *E. coli* are composite fibres with distinct fibrillar adhesive tips. Nature 1992;356:252–255.

280. Dodson KW, Pinkner JS, Rose T, Magnusson G, Hultgren SJ, Waksman G. Structural basis of the interaction of the pyelonephritic *E. coli* adhesin to its human kidney receptor. Cell 2001;105: 733–743.

281. Hanisch FG, Hacker J, Schroten H. Specificity of *S. fimbriae* on recombinant *Escherichia coli*: Preferential binding to gangliosides expressing NeuGc alpha (2–3)Gal and NeuAc alpha (2–8)NeuAc. Infect Immun 1993;61:2108–2115.

282. Duncan MJ, Mann EL, Cohen MS, Ofek I, Sharon N, Abraham SN. The distinct binding specificities exhibited by enterobacterial type 1 fimbriae are determined by their fimbrial shafts. J Biol Chem 2005;280:37707–37716.

283. Wellens A, Garofalo C, Nguyen H, Van Gerven N, Slattegard R, Hernalsteens JP, Wyns L, Oscarson S, De Greve H, Hultgren S, Bouckaert J. Intervening with urinary tract infections using anti-adhesives based on the crystal structure of the FimH-oligomannose-3 complex. PLoS One 2008;3:e2040.

284. Hung CS, Bouckaert J, Hung D, Pinkner J, Widberg C, DeFusco A, Auguste CG, Strouse R, Langermann S, Waksman G, Hultgren SJ. Structural basis of tropism of *Escherichia coli* to the bladder during urinary tract infection. Mol Microbiol 2002;44:903–915.

285. Stromberg N, Boren T. Actinomyces tissue specificity may depend on differences in receptor specificity for GalNAc beta-containing glycoconjugates. Infect Immun 1992;60:3268–3277.

286. Boren T, Falk P, Roth KA, Larson G, Normark S. Attachment of *Helicobacter pylori* to human gastric epithelium mediated by blood group antigens. Science 1993;262:1892–1895.

287. Hirmo S, Kelm S, Schauer R, Nilsson B, Wadstrom T. Adhesion of *Helicobacter pylori* strains to alpha-2,3-linked sialic acids. Glycoconj J 1996;13:1005–1011.

288. Sachse K, Pfutzner H, Heller M, Hanel I. Inhibition of *Mycoplasma bovis* cytadherence by a monoclonal antibody and various carbohydrate substances. Vet Microbiol 1993;36:307–316.

289. Murakami Y, Hanazawa S, Nishida K, Iwasaka H, Kitano S. *N*-Acetyl-D-galactosamine inhibits TNF-alpha gene expression induced in mouse peritoneal macrophages by fimbriae of Porphyromonas (Bacteroides) gingivalis, an oral anaerobe. Biochem Biophys Res Commun 1993;192:826–832.

290. Rosenstein IJ, Yuen CT, Stoll MS, Feizi T. Differences in the binding specificities of *Pseudomonas aeruginosa* M35 and *Escherichia coli* C600 for lipid-linked oligosaccharides with lactose-related core regions. Infect Immun 1992;60:5078–5084.

291. Wisniewski JP, Monsigny M, Delmotte FM. Purification of an alpha-L-fucoside-binding protein from *Rhizobium lupini*. Biochimie 1994;76:121–128.

292. Kitov PI, Lipinski T, Paszkiewicz E, Solomon D, Sadowska JM, Grant GA, Mulvey GL, Kitova EN, Klassen JS, Armstrong GD, Bundle DR. An entropically efficient supramolecular inhibition strategy for Shiga toxins. Angew Chem Int Ed Engl 2008;47:672–676.

293. Miyagawa A, Kasuya MCZ, Hatanaka K. Inhibitory effects of glycopolymers having globotriose and/or lactose on cytotoxicity of Shiga toxin 1. Carbohydr Polym 2007;67:260–264.

294. Dohi H, Nishida Y, Takeda T, Kobayashi K. Convenient use of non-malodorous thioglycosyl donors for the assembly of multivalent globo- and isoglobosyl trisaccharides. Carbohydr Res 2002;337:983–989.

295. Watanabe M, Matsuoka K, Kita E, Igai K, Higashi N, Miyagawa A, Watanabe T, Yanoshita R, Samejima Y, Terunuma D, Natori Y, Nishikawa K. Oral therapeutic agents with highly clustered globotriose for treatment of Shiga toxigenic *Escherichia coli* infections. J Infect Dis 2004;189:360–368.

296. Dohi H, Nishida Y, Furuta Y, Uzawa H, Yokoyama S, Ito S, Mori H, Kobayashi K. Molecular design and biological potential of galacto-type trehalose as a nonnatural ligand of Shiga toxins. Org Lett 2002;4:355–357.

297. Choi SK, Mammen M, Whitesides GM. Monomeric inhibitors of influenza neuraminidase enhance the hemagglutination inhibition activities of polyacrylamides presenting multiple C-sialoside groups. Chem Biol 1996;3:97–104.

298. Hiroshi Kamitakahara TS, Nishigori N, Suzuki Y, Kanie O, Wong C-H. A lysoganglioside/poly-l-glutamic acid conjugate as a picomolar inhibitor of influenza hemagglutinin. Angew Chem Int Ed 1998;37:1524–1528.
299. Wu WY, Jin B, Krippner GY, Watson KG. Synthesis of a polymeric 4-N-linked sialoside which inhibits influenza virus hemagglutinin. Bioorg Med Chem Lett 2000;10: 341–343.
300. Tsvetkov DE, Cheshev PE, Tuzikov AB, Chinarev AA, Pazynina GV, Sablina MA, Gambaryan AS, Bovin NV, Rieben R, Shashkov AS, Nifant'ev NE. Neoglycoconjugates based on dendrimer poly(aminoamides). Russ J Bioorg Chem 2002;28:470–486.
301. Landers JJ, Cao Z, Lee I, Piehler LT, Myc PP, Myc A, Hamouda T, Galecki AT, Baker JR, Jr. Prevention of influenza pneumonitis by sialic acid-conjugated dendritic polymers. J Infect Dis 2002;186:1222–1230.
302. Totani K, Kubota T, Kuroda T, Murata T, Hidari KI, Suzuki T, Suzuki Y, Kobayashi K, Ashida H, Yamamoto K, Usui T. Chemoenzymatic synthesis and application of glycopolymers containing multivalent sialyloligosaccharides with a poly(L-glutamic acid) backbone for inhibition of infection by influenza viruses. Glycobiology 2003;13:315–326.
303. Matsuoka K, Takita C, Koyama T, Miyamoto D, Yingsakmongkon S, Hidari KI, Jampangern W, Suzuki T, Suzuki Y, Hatano K, Terunuma D. Novel linear polymers bearing thiosialosides as pendant-type epitopes for influenza neuraminidase inhibitors. Bioorg Med Chem Lett 2007;17:3826–3830.
304. Honda T, Yoshida S, Arai M, Masuda T, Yamashita M. Synthesis and anti-influenza evaluation of polyvalent sialidase inhibitors bearing 4-guanidino-Neu5Ac2en derivatives. Bioorg Med Chem Lett 2002;12:1929–1932.
305. Marra A, Moni L, Pazzi D, Corallini A, Bridi D, Dondoni A. Synthesis of sialoclusters appended to calix[4]arene platforms via multiple azide-alkyne cycloaddition. New inhibitors of hemagglutination and cytopathic effect mediated by BK and influenza A viruses. Org Biomol Chem 2008;6:1396–1409.
306. Mann MC, Islam T, Dyason JC, Florio P, Trower CJ, Thomson RJ, von Itzstein M. Unsaturated N-acetyl-D-glucosaminuronic acid glycosides as inhibitors of influenza virus sialidase. Glycoconj J 2006;23:127–133.
307. Mendel DB, Tai CY, Escarpe PA, Li W, Sidwell RW, Huffman JH, Sweet C, Jakeman KJ, Merson J, Lacy SA, Lew W, Williams MA, Zhang L, Chen MS, Bischofberger N, Kim CU. Oral administration of a prodrug of the influenza virus neuraminidase inhibitor GS 4071 protects mice and ferrets against influenza infection. Antimicrob Agents Chemother 1998;42:640–646.
308. Finley JB, Atigadda VR, Duarte F, Zhao JJ, Brouillette WJ, Air GM, Luo M. Novel aromatic inhibitors of influenza virus neuraminidase make selective interactions with conserved residues and water molecules in the active site. J Mol Biol 1999;293:1107–1119.
309. Sakamoto J, Koyama T, Miyamoto D, Yingsakmongkon S, Hidari KI, Jampangern W, Suzuki T, Suzuki Y, Esumi Y, Hatano K, Terunuma D, Matsuoka K. Thiosialoside clusters using carbosilane dendrimer core scaffolds as a new class of influenza neuraminidase inhibitors. Bioorg Med Chem Lett 2007;17:717–721.

Ashish Kulkarni *was born in 1981 in Pandharpur, Maharashtra, India. He received his B.Tech. degree in Chemical Technology from the Institute of Chemical Technology, University of Mumbai (formerly known as U.D.C.T.), in 2003. Before joining Dr. Iyer's research group, he worked as a process engineer in NOCIL, a chemical company in India, for three years. Currently, he is a third year graduate student working in the development*

of fluorescent glycoconjugates for precise detection of pathogens. He is also developing glyconanoparticles for the inhibition of toxins and viruses.

Dr. Suri S. Iyer *is a synthetic chemist with research interests in carbohydrate chemistry, glycobiology, and biosensors. After receiving a masters in Organic Chemistry from the Indian Institute of Technology, Mumbai (formerly Bombay), he studied under the direction of Professor Malcolm Chisholm at Indiana University, Bloomington, Indiana. His graduate research focused on the synthesis of C-3 symmetric chiral complexes and its application toward the development of single site metal alkoxides for the ring opening polymerization of lactides and lactones. In 2000, he worked as a postdoctoral fellow at the Emory School of Medicine, Atlanta, GA, developing anticoagulant biomaterials. In 2002, Dr. Iyer joined the Biosensors Division, Los Alamos National Laboratory, Los Alamos, NM, where he worked on the synthesis of stable glycoconjugates for the capture of harmful pathogens. He started his first independent career in 2004 as an assistant professor at the University of Cincinnati. Currently, his group is developing high affinity synthetic glycans for capturing toxins, viruses, and bacteria.*

Dr. Alison Weiss *is a professor in the Department of Molecular Genetics, Biochemistry, and Microbiology at the University of Cincinnati. She received her A.B. degree in 1975 from Washington University and her M.S. in 1981 from the University of Washington in Seattle. She received her Ph.D. in 1983 from Stanford University, where her thesis advisor was Professor Stanley Falkow, who won the prestigious 2008 Lasker Award for medical research. She received a NIH predoctoral fellowship for her doctoral studies. From 1983 to 1985, she conducted her postdoctoral studies at the University of Virginia. Dr. Weiss started her first independent career as an associate professor in the Department of Microbiology and Immunology at Virginia Commonwealth University in 1985. She moved to the University of Cincinnati in 1993 and became a full Professor in 2000. Dr. Weiss has won numerous awards that include Damon Runyon–Walter Winchell Postdoctoral Fellowship in 1984, the Pew Scholar Award in Biomedical Sciences in 1987, and the American Society for Microbiology, Foundation Lectureship in 1990. She is in the editorial board of Infection and Immunity. Her research interests are in the field of bacterial toxins, specifically Pertussis and Shiga toxins.*